6096 *Inorg. Chem.* **2009**, *48*, 6096–6108
DOI: 10.1021/ic900463b

Inorganic Chemistry
Article

Switching between κ^2 and κ^3 Bis(pyrazol-1-yl)acetate Ligands by Tuning Reaction Conditions: Synthesis, Spectral, Electrochemical, Structural, and Theoretical Studies on Arene-Ru(II) Derivatives of Bis(azol-1-yl)acetate Ligands

Fabio Marchetti,*,[†] Claudio Pettinari,[†] Adele Cerquetella,[†] Augusto Cingolani,[†] Riccardo Pettinari,[†] Magda Monari,[‡] Riccardo Wanke,[§] Maxim L. Kuznetsov,[§] and Armando J. L. Pombeiro*,[§]

[†]*Dipartimento di Scienze Chimiche, Università degli Studi di Camerino, Via S. Agostino 1, 62032 Camerino MC, Italy,* [‡]*Dipartimento di Chimica "G. Ciamician", Università di Bologna, Via Selmi 2, I-40126 Bologna, Italy, and* [§]*Centro de Quìmica Estrutural, Complexo I, Instituto Superior Técnico, Av. Rovisco Pais, 1049-001 Lisbon, Portugal*

Received March 9, 2009

New (arene)ruthenium(II) derivatives containing neutral HL or anionic L^- ligands (arene = *p*-cymene or benzene, HL in general, in particular HL^1 = bis(pyrazol-1-yl)acetic acid and HL^2 = bis(3,5-dimethylpyrazol-1-yl)acetic acid) have been synthesized and analytically and spectrally characterized. The ligands in neutral form coordinate ruthenium in a chelating κ^2-*N,N'*-bidentate fashion affording 1:1 derivatives of formula [Ru(arene)(HL)Cl]Cl, where the inner Cl can be replaced by a phosphine. These derivatives show very high conductance values in water, due to the contribution of H_3O^+ produced by deprotonation of the $-$COOH fragment in HL ligands and consequent formation of 1:2 electrolytes such as $[Ru(arene)(\kappa^3\text{-}N,N',O\text{-}L)]Cl_2$ species. However, the remaining derivatives contain monoanion L^- ligands coordinating in the tripodal κ^3-*N,N',O*-tridentate fashion. The solid-state X-ray structure of the complex $[Ru(\eta^6\text{-}p\text{-cymene})(\kappa^3\text{-}N,N',O\text{-}L^1)]PF_6$ confirmed such behavior. The redox properties of those compounds have been investigated by cyclic voltammetry and controlled potential electrolysis, which, on the basis of their measured $Ru^{II/III}$ oxidation potentials, have allowed for the ordering of the HL and L^- ligands according to their electron-donor character. This is accounted for by DFT calculations, which show a relevant contribution of L ligand orbitals to the highest occupied molecular orbitals (HOMOs) when they are coordinated in the monoanionic tridentate form, while for derivatives containing neutral HL ligands, the main contribution to the HOMOs comes from orbitals of the metal and chlorine atoms, the overall contribution from the bidentate HL ligand orbitals being small. Values of the Lever electrochemical E_L ligand parameter (a measure of the net electron donor character of a ligand) have been estimated for the above and related acylpyrazolonate ligands, as well as for the η^6-coordinated benzene and cymene.

Introduction

The past few decades have witnessed a huge number of studies on mid-to-late d-metal complexes containing flexible polydentate donor ligands with tunable hapticity.[1] In fact, the need of new efficient and selective catalysts for a wide range of organic reactions has driven the research toward the design of polydentate ligands able to impose particular geometries on the catalytic metal centers, with the aim of finely tuning their ability to coordinate the reactants with the correct orientation and polarity for the subsequent reactions.[2] In this respect, the broad family of scorpionates is actually playing an important role as second- and third-generation ligands, providing fine control of the electronic and steric properties of the discrete or polymeric complex molecules and ions formed from these ligands.[3]

A new variation has been introduced by the synthesis of polydentate ligands containing different donor atoms, and among them the family of heteroscorpionates is actually playing a key role.[4] Special interest is devoted to bis(azolyl)

---

*To whom correspondence should be addressed. E-mail: fabio.marchetti@unicam.it (F.M.). For the electrochemical and computational data, E-mail: pombeiro@ist.utl.pt (A.J.L.P.).

(1) Pettinari, C.; Marchetti, F.; Drozdov, A. Higher Denticity Ligands. In *Comprehensive Coordination Chemistry II*; McCleverty, J. A., Meyer, T. J., Eds.; Elsevier: New York, 2003; Vol. 1, par. 1.11, pp 211−252.

(2) See, for example: (a) Alvarez, E.; Conejero, S.; Lara, P.; Lopez, J. A.; Paneque, M.; Petronilho, A.; Poveda, M. L.; del Rio, D.; Serrano, O.; Carmona, E. *J. Am. Chem. Soc.* **2007**, *129*, 14130. (b) Alvarez, E.; Conejero, S.; Paneque, M.; Petronilho, A.; Poveda, M. L.; Serrano, O.; Carmona, E. *J. Am. Chem. Soc.* **2006**, *128*, 13060. (c) Pettinari, C.; Marchetti, F.; Martini, D. Metal Complexes as Hydrogenation Catalysts. In *Comprehensive Coordination Chemistry II*; McCleverty, J. A., Meyer, T. J., Eds.; Elsevier: New York, 2003; Vol. *9*, chapter 9.2, pp 75-139.

acetic acids, which are a new class of N,N,O heteroscorpionate ligands, first introduced by Otero in 1999,[5] that can be "formally" thought of as bis(azol-1-yl)alkanes with an additional carboxylic fragment on the bridging carbon atom. In recent years, some papers dealing with Ru(II) and Ru(III) complexes containing bis(pyrazolyl)acetate ligands have been published,[6] in order to compare their structure and reactivity with those of similar ruthenium tris(pyrazolyl) borate derivatives, which show promising catalytic activity in ring-closing metathesis or ring-opening metathesis polymerization.[7]

Surprisingly, no attempts have been made until now to synthesize (arene)Ru(II) derivatives with bis(pyrazolyl)acetates, although the piano-stool half-sandwich (arene)Ru(II) fragment has been shown to possess the right geometry in order to induce a number of catalytic transformations, such as, for example, the highly efficient asymmetric hydrogen transfer on C=O-containing substrates reported by Noyori et al.[8]

Our interest in tripodal neutral and anionic N-donor ligands, such as first- and second-generation scorpionates, goes back a ways,[9] and we have recently reported on the synthesis and reactivity of (arene)Ru(II) (where arene = *p*-cymene or benzene) derivatives with bis(pyrazolyl)alkane ligands.[10]

As an extension of our previous studies, here we report on the reactions of (arene)Ru(II) acceptors (where arene = *p*-cymene or benzene) with bis(pyrazol-1-yl)acetic acid (HL^1) and the corresponding tetramethylated bis(3,5-dimethyl-pyrazol-1-yl)acetic acid (HL^2) and on the spectral, structural, and electrochemical characterization of the isolated complexes.

Experimental Section

Materials and Methods. All chemicals were purchased from Aldrich (Milwaukee, WI) and used as received. The ligands HL^1 (HL^1 = bis(pyrazol-1-yl)acetic acid) and HL^2 (HL^2 = bis(3,5-dimethylpyrazol-1-yl)acetic acid) were prepared according to literature methods.[6] The starting $[Ru(\eta^6\text{-benzene})Cl(\mu\text{-}Cl)]_2$ has been prepared according to literature methods.[11]

All of the reactions and manipulations were performed in the air. Solvent evaporations were always carried out under vacuum conditions using a rotary evaporator. The samples for microanalysis were dried in vacuo to a constant weight (20 °C, ca. 0.1 Torr). Elemental analyses (C, H, N) were performed in-house with a Fison Instrument 1108 CHNS-O elemental analyzer. IR spectra were recorded from 4000 to 200 cm^{-1} with a Perkin-Elmer Spectrum 100 FT-IR instrument. ^1H, ^{19}F, ^{31}P, and $^{13}C\{^1H\}$ NMR spectra were recorded on a 400 Mercury Plus Varian instrument operating at room temperature (400 MHz for ^1H, 100 MHz for ^{13}C, 162.1 MHz for ^{31}P, and 376.8 MHz for ^{19}F). H and C chemical shifts (δ) are reported in parts per million (ppm) from $SiMe_4$ (^1H and ^{13}C calibration by internal deuterium solvent lock), while P chemical shifts (δ) are reported in ppm versus 85% H_3PO_4. F chemical shifts are reported versus $CFCl_3$. Peak multiplicities are abbreviated: singlet, s; doublet, d; triplet, t; quartet, q; and multiplet, m. Melting points are uncorrected and were taken on an STMP3 Stuart scientific instrument and on a capillary apparatus. The electrical conductivity measurements (Λ_M, reported as Ω^{-1} cm^2 mol^{-1}) of acetonitrile and water solutions of the complexes were taken with a Crison CDTM 522 conductimeter at room temperature. The pH measurements of aqueous solutions of derivatives were performed with a Crison pH-Meter basic 20+. The positive and negative electrospray mass spectra were obtained with a Series 1100 MSI detector HP spectrometer, using an acetonitrile mobile phase. Solutions (3 mg/mL) for electrospray ionization mass spectrometry (ESI-MS) were prepared using reagent-grade acetonitrile. For the ESI-MS data, mass and intensities were compared to those calculated using IsoPro Isotopic Abundance Simulator, version 2.1.[12] Peaks containing ruthenium(II) ions are identified as the center of an isotopic cluster.

Electrochemistry. The electrochemical experiments were carried out on an EG&G PAR 273A potentiostat/galvanostat connected to a personal computer through a GPIB interface. Cyclic voltammetry (CV) studies were undertaken in a two-compartment three-electrode cell, with platinum disk working (d = 0.5 mm) and counter electrodes. A Luggin capillary connected to a silver-wire pseudo-reference electrode was used to control the working electrode potential. Controlled potential electrolyses (CPE) were carried out in a two-compartment three-electrode cell with platinum-gauze working and counter electrodes in compartments separated by a glass frit; a Luggin capillary, probing the working electrode, was connected to a silver-wire pseudo-reference electrode. The solutions were saturated with N_2 by bubbling this gas before each run, and the oxidation

---

(3) (a) Reger, D. L.; Watson, R. P.; Gardinier, J. R.; Smith, M. D. *Inorg. Chem.* **2004**, *43*, 6609. (b) Reger, D. L.; Gardinier, J. R.; Semeniuc, R. F.; Smith, M. D. *J. Chem. Soc., Dalton Trans.* **2003**, 1712. (c) Reger, D. L.; Watson, R. P.; Smith, M. D.; Pellechia, P. J. *Organometallics* **2005**, *24*, 1544. (d) Reger, D. L.; Watson, R. P.; Smith, M. D.; Pellechia, P. J. *Organometallics* **2006**, *25*, 743. (e) Reger, D. L.; Gardinier, J. R.; Grattan, T. C.; Smith, M. R.; Smith, M. D. *New J. Chem.* **2003**, *27*, 1670. (f) Reger, D. L.; Semeniuc, R. F.; Smith, M. D. *J. Organomet. Chem.* **2003**, *666*, 87. (g) Reger, D. L.; Brown, K. J.; Smith, M. D. *J. Organomet. Chem.* **2002**, *658*, 50. (h) Reger, D. L.; Wright, T. D.; Semeniuc, R. F.; Grattan, T. C.; Smith, M. D. *Inorg. Chem.* **2001**, *40*, 6212. (i) Reger, D. L.; Brown, K. J.; Gardinier, J. R.; Smith, M. D. *Organometallics* **2003**, *22*, 4973. (j) Reger, D. L.; Gardinier, J. R.; Smith, M. D. *Polyhedron* **2004**, *23*, 291. (k) Reger, D. L.; Watson, R. P.; Smith, D.; Pellechia, P. J. *Cryst. Growth Des.* **2007**, *7*, 1163. (l) Reger, D. L.; Foley, E. A.; Semeniuc, R. F.; Smith, M. D. *Inorg. Chem.* **2007**, *46*, 11345. (m) Reger, D. L.; Foley, E. A.; Smith, M. D. *Inorg. Chem.* **2009**, *48*, 936.

(4) Pettinari, C.; Santini, C. Polypyrazolylborates and Scorpionate Ligands. In *Comprehensive Coordination Chemistry II*; McCleverty, J. A., Meyer, T. J., Eds.; Elsevier, 2003, Vol. 1, chapter 1.10, pp 159−210.

(5) Otero, A.; Fernández-Baeza, J.; Tejeda, J.; Antiñolo, A.; Carrillo-Hermosilla, F.; Díez-Barra, E.; Lara-Sánchez, A.; Fernández-López, M.; Lanfranchi, M.; Pellinghelli, M. A. *J. Chem. Soc., Dalton Trans.* **1999**, 3537.

(6) (a) López-Hernández, A.; Müller, R.; Kopf, H.; Burzlaff, N. *Eur. J. Inorg. Chem.* **2002**, 671. (b) Hegelmann, I.; Burzlaff, N. *Eur. J. Inorg. Chem.* **2003**, 409. (c) Müller, R.; Hübner, E.; Burzlaff, N. *Eur. J. Inorg. Chem.* **2004**, 2151. (d) Ortiz, M.; Díaz, A.; Cao, R.; Suardíaz, R.; Otero, A.; Antiñolo, A.; Fernández-Baeza, J. *Eur. J. Inorg. Chem.* **2004**, 3353. (e) Ortiz, M.; Díaz, A.; Cao, R.; Otero, A.; Antiñolo, A.; Fernández-Baeza, J. *Inorg. Chim. Acta* **2004**, *357*, 19. (f) Peters, Liv.; Burzlaff, N. *Polyhedron* **2004**, *23*, 245. (g) Kopf, H.; Pietraszuk, C.; Hübner, E.; Burzlaff, N. *Organometallics* **2006**, *25*, 2533. (h) Kopf, H.; Holzberger, B.; Pietraszuk, C.; Hübner, E.; Burzlaff, N. *Organometallics* **2008**, *27*, 5894. (i) Tampier, S.; Müller, R.; Thorn, A.; Hübner, E.; Burzlaff, N. *Inorg. Chem.* **2008**, *47*, 9624.

(7) (a) Katayama, H.; Yoshida, T.; Ozawa, F. *J. Organomet. Chem.* **1998**, *562*, 203. (b) Sanford, M. S.; Henling, L. M.; Grubbs, R. H. *Organometallics* **1998**, *17*, 5384. (c) Bruneau, C.; Dixneuf, P. H. *Acc. Chem. Res.* **1999**, *32*, 311–323. (d) Fürstner, A. *Angew. Chem., Int. Ed.* **2000**, *39*, 3012.

(8) (a) Hashiguchi, S.; Fujii, A.; Takehara, J.; Ikariya, T.; Noyori, R. *J. Am. Chem. Soc.* **1995**, *117*, 7562. (b) Fujii, A.; Hashiguchi, S.; Uematsu, N.; Ikariya, T.; Noyori, R. *J. Am. Chem. Soc.* **1996**, *118*, 2521.

(9) See, for example: Pettinari, C.; Pettinari, R.; Marchetti, F.; Macchioni, A.; Zuccaccia, D.; Skelton, B. W.; White, A. H. *Inorg. Chem.* **2007**, *46*, 896 and references reported therein. Carmona, E.; Cingolani, A.; Marchetti, F.; Pettinari, C.; Pettinari, R.; Skelton, B. W.; White, A. H. *Organometallics* **2003**, *22*, 2820 and references reported therein.

(10) Marchetti, F.; Pettinari, C.; Pettinari, R.; Cerquetella, A.; Di Nicola, C.; Macchioni, A.; Zuccaccia, D.; Monari, M.; Piccinelli, F. *Inorg. Chem.* **2008**, *47*, 11593.

(11) (a) Bennett, M. A.; Huang, T. N.; Matheson, T. W.; Smith, A. K. *Inorg. Synth.* **1982**, *21*, 74. (b) Bennett, M. A.; Matheson, T. W.; Robertson, G. B.; Smith, A. K.; Tucker, P. A. *Inorg. Chem.* **1980**, *19*, 1014.

(12) Senko, M. W. *IsoPro Isotopic Abundance Simulator*, Vol. *2.1*; National High Field Laboratory, Los Alamos National Laboratory: Los Alamos, NM.

potentials of the complexes were measured by CV, in the presence of ferrocene as an internal standard. The redox potential values are initially quoted relative to the saturated calomel electrode (SCE) by using the $[Fe(\eta^5\text{-}C_5H_5)_2]^{0/+}$ ($E^{ox}_{1/2}$ = 0.450 V vs SCE) redox couple in the 0.2 M $[Bu_4N][BF_4]/CH_3CN$ solution.[13] They have been converted to the normal hydrogen electrode (NHE) by adding 0.245 V.

Computational Details. The full geometry optimization of the complexes has been carried out in Cartesian coordinates at the DFT level of theory using Becke's three-parameter hybrid exchange functional[14] in combination with the gradient-corrected correlation functional of Lee, Yang, and Parr[15] (B3LYP) with the help of the Gaussian 98[16] program package. The restricted approximations for the structures with closed electron shells and the unrestricted methods for the structures with open electron shells have been employed. Symmetry operations were not applied for all structures. A quasi-relativistic Stuttgart pseudopotential described 28 core electrons, and the appropriate contracted basis set (8s7p6d)/[6s5p3d][17] for the ruthenium atom and the 6-31G(d) basis set for other atoms were used. The Hessian matrix was calculated analytically for the nonoxidized species to prove the location of correct minima (no "imaginary" frequencies were found). The experimental X-ray geometries of **10** and **15** were taken as a basis for the initial geometries of the optimization processes. The analysis of the metal−ligand bonding nature and degree of the ligand-to-metal donation have been performed for some closed-shell structures using the CDA method of Dapprich and Frenking[18a] with the help of the CDA 2.1 program.[18b] This method describes the bonding in a complex as a result of interactions of molecular orbitals (MOs) of a ligand and a metal fragment. Four types of such interactions are considered, that is, the d-term corresponding to the ligand-to-metal donation, the b-term related to the metal-to-ligand back-donation, the r-term characterizing the repulsion of the occupied orbitals of two fragments, and the nonclassical Δ-term corresponding to the interaction of unoccupied MOs of the fragments.

Syntheses of Complexes. $[Ru(\eta^6\text{-}p\text{-cymene})(\kappa^2\text{-}N,N'\text{-}HL^1)Cl]Cl$ (1). $[Ru(\eta^6\text{-}p\text{-cymene})Cl(\mu\text{-}Cl)]_2$ (0.306 g, 0.5 mmol) was dissolved in methanol (20 mL) and stirred for 30 min; then, HL^1 (0.192 g, 1.0 mmol) was added to the red solution, which immediately changed to orange. After 24 h of stirring at room temperature, the clear orange solution was evaporated to dryness and redissolved in diethyl ether (5 mL), from which a precipitate slowly formed, which was filtered off and dried under reduced pressure. The powder was identified as derivative **1**. It is only slightly soluble in acetonitrile and very soluble in water, methanol, chloroform, and DMSO. Yield: 85%. Mp > 220 °C dec. Anal. calcd for $C_{18}H_{22}Cl_2N_4O_2Ru$: C, 43.38; H, 4.45; N, 11.24. Found: C. 43.64; H, 4.39; N, 11.09%. Λ_m (H_2O, 298 K, 10^{-4} mol/L): 317 Ω^{-1} cm^2 mol^{-1}. IR (nujol, cm^{-1}): 3350br $\nu(O-H)$, 3103m $\nu(C_{arom}-H)$, 1751s $\nu_{asym}(COO)$, 1658m $\nu_{sym}(COO)$, 1508m $\nu(C{=}N + C{=}C)$, 297s $\nu(Ru-Cl)$. ^1H (D_2O): δ 1.06d (6H, $CH_3-C_6H_4-CH(CH_3)_2$), 2.10s (3H, $CH_3-C_6H_4-CH(CH_3)_2$), 2.88m (1H, $CH_3-C_6H_4-CH(CH_3)_2$), 5.79d, 6.12d (4H, AA′BB′ system, $CH_3-C_6H_4-CH(CH_3)_2$), 6.53t (2H, H_4 of HL^1), 6.90s (C−*H* of HL^1), 7.92d (2H, H_5 of HL^1), 8.54d (2H, H_3 of HL^1), COO*H* of HL^1 not observed. $^{13}C\{^1H\}$ (D_2O): δ 20.14 (s, $CH_3-C_6H_4-CH(CH_3)_2$), 24.35 (s, $CH_3-C_6H_4-CH(CH_3)_2$), 33.37 (s, $CH_3-C_6H_4-CH(CH_3)_2$), 74.30 (s, *C*H of HL^1), 85.71, 88.75, 105.1, 106.4 (s, $CH_3-C_6H_4-CH(CH_3)_2$), 112.01 (s, C_4 of HL^1), 136.99 (s, C_5 of HL^1), 149.58 (s, C_3 of HL^1), 170.32 (s, *C*OOH of HL^1). ^1H ($CDCl_3$): δ 1.37d (6H, $CH_3-C_6H_4-CH(CH_3)_2$), 2.09s (3H, $CH_3-C_6H_4-CH(CH_3)_2$), 2.88m (1H, $CH_3-C_6H_4-CH(CH_3)_2$), 5.37d, 5.74d (4H, AA′BB′ system, $CH_3-C_6H_4-CH(CH_3)_2$), 6.52t (2H, H_4 of HL^1), 6.90s (1H, C*H* of HL^1), 7.81d (2H, H_5 of HL^1), 8.80d (2H, H_3 of HL^1), 10.80br (1H, COO*H* of HL^1).

ESI-MS (+) H_2O (*m*/*z*, relative intensity %): 427 [100] $[Ru(cymene)(L^1)]^+$.

$[Ru(\eta^6\text{-benzene})(\kappa^2\text{-}N,N'\text{-}HL^1)Cl]Cl$ (2). Derivative **2** was prepared following a procedure similar to that reported for **1** by using $[Ru(\eta^6\text{-benzene})Cl(\mu\text{-}Cl)]_2$ (0.250 g, 0.5 mmol) and HL^1 (0.192 g, 1.0 mmol) in acetonitrile (20 mL), from which a precipitate slowly formed, which was filtered off, dried, and shown to be derivative **2**. It is quite soluble in water, chloroform, and DMSO. Yield: 65%. Mp > 250 °C dec. Anal. calcd for $C_{14}H_{14}Cl_2N_4O_2Ru$: C, 38.02; H, 3.19; N, 12.67. Found: C. 38.29; H, 3.30; N, 12.59%. Λ_m (H_2O, 298 K, 10^{-4} mol/L): 332 Ω^{-1} cm^2 mol^{-1}. IR (nujol, cm^{-1}): 3400br $\nu(O-H)$, 3131m $\nu(C_{arom}-H)$, 1726m $\nu_{asym}(COO)$, 1509m $\nu(C{=}N+C{=}C)$, 282s $\nu(Ru-Cl)$. ^1H (D_2O): δ 6.13s (6H, C_6H_6), 6.53t (2H, H_4 of HL^1), 6.90s (1H, C−*H* of HL^1), 7.93d (2H, H_5 of HL^1), 8.61d (2H, H_3 of HL^1), COO*H* of HL^1 not observed. $^{13}C\{^1H\}$ (D_2O): δ 74.14 (s, *C*H of HL^1), 88.53 (s, C_6H_6), 111.86 (s, C_4 of HL^1), 136.85 (s, C_5 of HL^1), 149.82 (s, C_3 of HL^1), 169.70 (s, *C*OOH of HL^1). ESI-MS (+) H_2O (*m*/*z*, relative intensity %): 371 [100] $[Ru(benzene)(L^1)]^+$. ESI-MS (+) CH_3CN (*m*/*z*, relative intensity %): 371 [100] $[Ru(benzene)(L^1)]^+$, 407 [100] $[Ru(benzene)(L^1)(H_2O)_2]^+$.

$[Ru(\eta^6\text{-}p\text{-cymene})(\kappa^2\text{-}N,N'\text{-}HL^1)Cl]BF_4$ (3). Derivative **1** (0.498 g, 1.0 mmol) was dissolved in acetonitrile (20 mL), and $AgBF_4$ (0.195 g, 1.0 mmol) was added to the red solution, which immediately changed to orange. A colorless precipitate was formed. After 2 h of stirring at room temperature, the mixture was filtered to remove silver chlorid; the solvent was then removed in vacuo and the residue dried under reduced pressure. The powder was identified as derivative **3**. It is soluble in acetonitrile, methanol, and acetone. It is slightly soluble in water and chloroform. Yield: 79%. Mp > 250 °C dec. Anal. calcd for $C_{18}H_{22}BClF_4N_4O_2Ru$: C, 39.33; H, 4.03; N, 10.19. Found: C, 39.58; H, 4.14; N, 10.05%. Λ_m (acetonitrile, 298 K, 10^{-4} mol/L): 120 Ω^{-1} cm^2 mol^{-1}. Λ_m (H_2O, 298 K, 10^{-4} mol/L): 355 Ω^{-1} cm^2 mol^{-1}. IR (nujol, cm^{-1}): 3450br $\nu(O-H)$, 3103m $\nu(C_{arom}-H)$, 1756 $\nu_{asym}(COO)$, 1671m $\nu_{sym}(COO)$, 1508m $\nu(C{=}N + C{=}C)$, 524m, 977m, 1025m $\nu(BF_4)$. ^1H (CD_3CN): δ, 1.32d (6H, $CH_3-C_6H_4-CH(CH_3)_2$), 1.96s (3H, $CH_3-C_6H_4-CH(CH_3)_2$), 2.92m (1H, $CH_3-C_6H_4-CH(CH_3)_2$), $CH(CH_3)_2$), 5.47d, 5.90d (4H, AA′BB′ system, $CH_3-C_6H_4-CH(CH_3)_2$), 6.66t (2H, H_4 of HL^1), 6.49s (C−*H* of HL^1), 8.04d (2H, H_5 of HL^1), 8.56d (2H, H_3 of HL^1), COO*H* of HL^1 not observed. $^{13}C\{^1H\}$ (CD_3CN): δ 18.72 (s, $CH_3-C_6H_4-CH(CH_3)_2$), 22.52 (s, $CH_3-C_6H_4-CH(CH_3)_2$), 31.50 (s, $CH_3-C_6H_4-CH(CH_3)_2$), 72.64 (s, *C*H of HL^1), 83.61, 87.25, 104.91, 110.41 (s, $CH_3-C_6H_4-CH(CH_3)_2$), 118.41 (s, C_4 of HL^1), 138.74 (s, C_5 of HL^1), 150.67 (s, C_3 of HL^1), 165.26 (s, *C*OOH of HL^1). $^{19}F\{^1H\}$ (MeCN): δ −151.85, −151.80. ESI-MS (+) H_2O (*m*/*z*, relative intensity %): 427 [100]

---

[13] Pombeiro, A. J. L.; Guedes da Silva, M. F. C.; Lemos, M. A. N. D. A. *Coord. Chem. Rev.* **2001**, *80*, 219.

[14] Becke, A. D. *J. Chem. Phys.* **1993**, *98*, 5648.

[15] Lee, C.; Yang, W.; Parr, R. G. *Phys. Rev.* **1988**, *B37*, 785.

[16] Frisch, M. J.; Trucks, G. W.; Schlegel, H. B.; Scuseria, G. E.; Robb, M. A.; Cheeseman, J. R.; Zakrzewski, V. G.; Montgomery, J. A., Jr.; Stratmann, R. E.; Burant, J. C.; Dapprich, S.; Millam, J. M.; Daniels, A. D.; Kudin, K. N.; Strain, M. C.; Farkas, O.; Tomasi, J.; Barone, V.; Cossi, M.; Cammi, R.; Mennucci, B.; Pomelli, C.; Adamo, C.; Clifford, S.; Ochterski, J.; Peterson, G. A.; Ayala, P. Y.; Cui, Q.; Morokuma, K.; Malick, D. K.; Rabuck, A. D.; Raghavachari, K.; Foresman, J. B.; Cioslowski, J.; Ortiz, J. V.; Baboul, A. G.; Stefanov, B. B.; Liu, G.; Liashenko, A.; Piskorz, P.; Komaromi, I.; Gomperts, R.; Martin, R. L.; Fox, D. J.; Keith, T.; Al-Laham, M. A.; Peng, C. Y.; Nanayakkara, A.; Challacombe, M.; Gill, P. M. W.; Johnson, B.; Chen, W.; Wong, M. W.; Andres, J. L.; Gonzalez, C.; Head-Gordon, M.; Replogle, E. S.; Pople, J. A. *Gaussian 98*, revision A.9; Gaussian, Inc.: Pittsburgh PA, 1998.

[17] Andrae, D.; Haeussermann, U.; Dolg, M.; Stoll, H.; Preuss, H. *Theor. Chim. Acta* **1990**, *77*, 123.

[18] (a) Dapprich, S.; Frenking, G. *J. Phys. Chem.* **1995**, *99*, 9352. (b) Dapprich, S.; Frenking, G. *CDA 2.1*; Universität Marburg: Marburg, Germany, 1995. The program is available via: ftp.chemie.uni-marburg.de/pub/cda (accessed June 2009).

[Ru(cymene)(L^1)]$^+$. ESI-MS (+) CH_3CN (*m*/*z*, relative intensity %): 427 [100] [Ru(cymene)(L^1)]$^+$.

[Ru(η^6-benzene)(κ^2-*N*,*N*′-HL^1)Cl]BF$_4$ (4). Derivative **4** was prepared following a procedure similar to that reported for **3** by using derivative **2** (0.442 g, 1.0 mmol) and $AgBF_4$ (0.195 g, 1.0 mmol). It is soluble in acetonitrile, methanol, water, and acetone. Yield: 79%. Mp 76−85 °C. Anal. calcd for $C_{14}H_{14}BClF_4N_4O_2Ru$: C, 34.07; H, 2.86; N, 11.35. Found: C, 33.88; H, 2.76; N, 11.18%. Λ_m (acetonitrile, 298 K, 10^{-4} mol/L): 122 Ω^{-1} cm^2 mol^{-1}. Λ_m (H_2O, 298 K, 10^{-4} mol/L): 369 Ω^{-1} cm^2 mol^{-1}. IR (nujol, cm^{-1}): 3550br ν(O−H), 3103m ν(C$_{arom}$−H), 1739 ν_{asym}(COO), 1662m ν_{sym}(COO), 1509m ν(C=N + C=C), 520m, 1056m ν(BF$_4$). ^{1}H (MeCN): δ 6.15s (6H, C_6H_6), 6.67t (2H, H_4 of HL^1), 7.41s (C−*H* of HL^1), 8.06d (2H, H_5 of HL^1), 8.71d (2H, H_3 of HL^1), COO*H* of HL^1 not observed. ^{13}C{^{1}H} (MeCN): δ 72.41, 73.09 (s, *C*H of HL^1), 86.79, 87.17, 87,86, 87.95, 87.98, 89.96 (s, C_6H_6), 109.57, 109.78, 110.07, 110.80 (s, C_4 of HL^1), 134.95, 138.04, 138.33, 139.66 (s, C_5 of HL^1), 148.00, 150.47, 151.30, 151.73 (s, C_3 of HL^1), 165.30 (s, *C*OOH of HL^1). ^{19}F{^{1}H} (MeCN): δ −151.90, −151.85, −151.80. ESI-MS (+) H_2O (*m*/*z*, relative intensity %): 371 [100] [Ru(benzene)(L^1)]$^+$. ESI-MS (+) CH_3CN (*m*/*z*, relative intensity %): 371 [100] [Ru(benzene)(L^1)]$^+$, 407 [100] [Ru(benzene)(L^1)(H_2O)$_2$]$^+$.

[Ru(η^6-*p*-cymene)(κ^2-*N*,*N*′-HL^1)Cl]PF$_6$ (5). Derivative **1** (0.498 g, 1.0 mmol) was dissolved in acetonitrile (20 mL); then, NH_4PF_6 (0.163 g, 1.0 mmol) was added to the red solution, which immediately changed to orange. After 1−2 h of stirring at room temperature, the solution was filtered to remove ammonium chloride; the solvent was removed in vacuo and the residue dried under reduced pressure. The powder was identified as derivative **5**. It is soluble in DMSO, water, methanol, acetonitrile, and chloroform. Yield: 92%. Mp 90−97 °C. Anal. calcd for $C_{18}H_{22}F_6N_4O_2PRu$: C, 35.57; H, 3.65; N, 9.22. Found: C, 35.30; H, 3.54; N, 8.98%. Λ_m (acetonitrile, 298 K, 10^{-4} mol/L): 127 Ω^{-1} cm^2 mol^{-1}. Λ_m (H_2O, 298 K, 10^{-4} mol/L): 375 Ω^{-1} cm^2 mol^{-1}. IR (nujol, cm^{-1}): 3600br ν(O−H), 3146m ν (C$_{arom}$−H), 1671s ν_{asym}(COO), 1508m ν(C=N + C=C), 833vs, 556s ν(PF$_6$), 287s ν(Ru−Cl). ^{1}H (D_2O): δ 1.05d (6H, $CH_3-C_6H_4-CH(CH_3)_2$), 2.12s (3H, $CH_3-C_6H_4-CH(CH_3)_2$), 2.88m (1H, $CH_3-C_6H_4-CH(CH_3)_2$), 5.79d, 5.81d (4H, AA′BB′ system, $CH_3-C_6H_4-CH(CH_3)_2$), 6.54t (2H, H_4 of HL^1), 7.93d (2H, H_5 of HL^1), 8.56d (2H, H_3 of HL^1), 6.92s (C−*H* of HL^1), COO*H* of HL^1 not observed. ^{13}C{^{1}H} (D_2O): δ n.o. (s, $CH_3-C_6H_4-CH(CH_3)_2$), 24.33 (s, $CH_3-C_6H_4-CH(CH_3)_2$), n.o. (s, $CH_3-C_6H_4-CH(CH_3)_2$), n.o. (s, *C*−H of HL^1), 85.70, 88.75 (s, AA′BB′ system, $CH_3-C_6H_4-CH(CH_3)_2$), 112.01 (s, C_4 of HL^1), 136.94 (s, C_5 of HL^1), 149.56 (s, C_3 of HL^1), *C*OOH of HL^1 not observed. ^{19}F{^{1}H} (CD_3CN): δ −74.19, −72.32. ESI-MS (+) H_2O (*m*/*z*, relative intensity %): 427 [100] [Ru(cymene)(L^1)]$^+$. ESI-MS (+) CH_3CN (*m*/*z*, relative intensity %): 427 [100] [Ru(cymene)(L^1)]$^+$.

[Ru(η^6-*p*-cymene)(κ^2-*N*,*N*′-HL^2)Cl]Cl (6). Derivative **6** was prepared following a procedure similar to that reported for **1** by using [Ru(η^6-*p*-cymene)Cl(μ-Cl)]$_2$ (0.306 g, 0.5 mmol) and HL^2 (0.248 g, 1.0 mmol). It is slightly soluble in acetonitrile and very soluble in water, methanol, chloroform, and DMSO. Yield: 78%. Mp 132−142 °C. Anal. calcd for $C_{22}H_{30}Cl_2N_4O_2Ru$: C, 47.66; H, 5.45; N, 10.10. Found: C. 47.41; H, 5.64; N, 9.81%. Λ_m (H_2O, 298 K, 10^{-4} mol/L): 269 Ω^{-1} cm^2 mol^{-1}. IR (nujol, cm^{-1}): 3350br ν(O−H), 3103m ν(C$_{arom}$−H), 1723m ν_{asym}(COO), 1662m ν_{sym}(COO), 1508m ν(C=N + C=C), 280m ν(Ru−Cl). ^{1}H (D_2O): δ, 1.04d (6H, $CH_3-C_6H_4-CH(CH_3)_2$), 2.03s (3H, $CH_3-C_6H_4-CH(CH_3)_2$), 2.30s (3H, C5−CH_3 of HL^2), 2.37s (3H, C3−CH_3 of HL^2), 2.85m (1H, $CH_3-C_6H_4-CH(CH_3)_2$), 5.72d, 5.85d (4H, AA′BB′ system, $CH_3-C_6H_4-CH(CH_3)_2$), 6.16s (2H, H_4 of HL^2), 6.59s (C−*H* of HL^2), COO*H* of HL^2 not observed. ^{13}C{^{1}H} (D_2O): δ 11.06, 11.17 (s, C5−CH_3 of HL^2), 14.84, 16.08 (s, C3−CH_3 of HL^2), 17.87, 18.28 (s, $CH_3-C_6H_4-CH(CH_3)_2$), 22.07, 22.13 (s, $CH_3-C_6H_4-CH(CH_3)_2$), 31.24 (s, $CH_3-C_6H_4-CH(CH_3)_2$), 67.23, 76.72 (s, *C*−H of HL^2), 81.46, 82.12, 102.54, 104.55 (s, $CH_3-C_6H_4-CH(CH_3)_2$), 108.79, 109.93 (s, C_4 of HL^2), 146.37, 147.08 (s, C_5 of HL^2), 155.35, 156.64 (s, C_3 of HL^2), 168.33 (s, *C*OOH of HL^2). ^{1}H ($CDCl_3$): δ 1.21d (6H, $CH_3-C_6H_4-CH(CH_3)_2$), 2.15s (3H, $CH_3-C_6H_4-CH(CH_3)_2$), 2.51s (3H, C5−CH_3 of HL^2), 2.58s (3H, C3−CH_3 of HL^2), 2.92m (1H, $CH_3-C_6H_4-CH(CH_3)_2$), 5.71d, 5.91d (4H, AA′BB′ system, $CH_3-C_6H_4-CH(CH_3)_2$), 6.15s (2H, H_4 of HL^2), 6.76s (C−*H* of HL^2), 7.40br (1H, COO*H* of HL^2). ^{13}C{^{1}H} ($CDCl_3$): δ 12.89 (sbr, C5−CH_3 of HL^2), 16.67 (s, C3−CH_3 of HL^2), 19.14, 20.95 (s, $CH_3-C_6H_4-CH(CH_3)_2$), 23.22, 24.09 (s, $CH_3-C_6H_4-CH(CH_3)_2$), 31.44, 33.68 (s, $CH_3-C_6H_4-CH(CH_3)_2$), 66.49 (sbr, *C*−H of HL^2), 84.28, 86.45, 103.16, 107.29 (sbr, $CH_3-C_6H_4-CH(CH_3)_2$), 109.77 (s, C_4 of HL^2), 145.54 (s, C_5 of HL^2), 156.70 (s, C_3 of HL^2), 163.94 (s, *C*OOH of HL^2). ESI-MS (+) H_2O (*m*/*z*, relative intensity %): 483 [100] [Ru(cymene)(L^2)]$^+$, 519 [10] [Ru(cymene)(HL^2)Cl]$^+$. ESI-MS (+) CH_3CN (*m*/*z*, relative intensity %): 475 [40] [Ru(cymene)(H_2C(3,5-Me$_2$pz)$_2$)Cl]$^+$, 519 [30] [Ru(cymene)(HL^2)Cl]$^+$.

[Ru(η^6-*p*-cymene)(κ^2-*N*,*N*′-HL^2)Cl]BF$_4$ (7). Derivative **7** was prepared following a procedure similar to that reported for **7** by using derivative **6** (0.554 g, 1.0 mmol) and $AgBF_4$ (0.195 g, 1.0 mmol). It is very soluble in acetonitrile, methanol, acetone, chloroform, and water. Yield: 79%. Mp 84−87 °C. Anal. calcd for $C_{22}H_{30}BClF_4N_4O_2Ru$: C, 43.62; H, 4.99; N, 9.25. Found: C, 43.53; H, 5.06; N, 9.13%. Λ_m (acetonitrile, 298 K, 10^{-4} mol/L): 118 Ω^{-1} cm^2 mol^{-1}. Λ_m (H_2O, 298 K, 10^{-4} mol/L): 279 Ω^{-1} cm^2 mol^{-1}. IR (nujol, cm^{-1}): 3650br ν(O−H), 3103m ν(C$_{arom}$−H), 1743 ν_{asym}(COO), 1629m ν_{sym}(COO), 1508m ν(C=N + C=C), 520m, 1055m ν(BF$_4$). ^{1}H ($CDCl_3$): δ 1.21d (6H, $CH_3-C_6H_4-CH(CH_3)_2$), 2.16s (3H, $CH_3-C_6H_4-CH(CH_3)_2$), 2.49s (3H, C5−CH_3 of HL^2), 2.53s (3H, C3−CH_3 of HL^2) 2.88m (1H, $CH_3-C_6H_4-CH(CH_3)_2$), 5.68d, 5.85d (4H, AA′BB′ system, $CH_3-C_6H_4-CH(CH_3)_2$), 6.17s (2H, H_4 of HL^2), 6.89s (C−*H* of HL^2). ^{13}C{^{1}H} ($CDCl_3$): δ 12.13, (s, C5−CH_3 of HL^2), 16.80, (s, C3−CH_3 of HL^2), $CH_3-C_6H_4-CH(CH_3)_2$ not observed, 23.16, 24.26 (s, $CH_3-C_6H_4-CH(CH_3)_2$), 31.80 (s, $CH_3-C_6H_4-CH(CH_3)_2$), 66.07, (s, *C*−H of HL^2), $CH_3-C_6H_4-CH(CH_3)_2$ not observed, 110.06 (s, C_4 of HL^2), 146.55 (s, C_5 of HL^2), 157.29 (s, C_3 of bdmpzaH), *C*OOH of HL^2 not observed. ^{19}F{^{1}H} ($CDCl_3$): δ −150.18, −151.90. ESI-MS (+) H_2O (*m*/*z*, relative intensity %): 483 [100] [Ru(cymene)(L^2)]$^+$, 519 [10] [Ru(cymene)(HL^2)Cl]$^+$. ESI-MS (+) CH_3CN (*m*/*z*, relative intensity %): 475 [40] [Ru(cymene)(H_2C(3,5-Me$_2$pz)$_2$)Cl]$^+$, 519 [30] [Ru(cymene)(HL^2)Cl]$^+$.

[Ru(η^6-*p*-cymene)(κ^2-*N*,*N*′-HL^2)(PPh$_3$)]Cl$_2$ (8). Derivative **6** (0.554 g, 1.0 mmol) was dissolved in chloroform (10 mL), and PPh_3 (0.262 g, 1.0 mmol) was added to the red solution, which immediately changed to orange. After 24 h of stirring at room temperature, the clear orange solution was evaporated to dryness and redissolved in diethyl ether (5 mL) and left in a freezer at 4 °C. A yellow precipitate slowly formed, which was identified as derivative **8**. It is very soluble in water, methanol, and chloroform. Yield: 79%. Mp 83−88 °C. Anal. calcd for $C_{40}H_{45}Cl_2N_4O_2PRu$: C, 58.82; H, 5.55; N, 6.86. Found: C, 58.97; H, 5.47; N, 6.64%. Λ_m (H_2O, 298 K, 10^{-4} mol/L): 191 Ω^{-1} cm^2 mol^{-1}. IR (nujol, cm^{-1}): 3380br ν(O−H), 3103m ν(C$_{arom}$−H), 1703 ν_{asym}(COO), 1663m ν_{sym}(COO), 1508m ν(C=N + C=C), 541m, 510s, 500m ν(PPh$_3$). ^{1}H ($CDCl_3$): δ 1.21d (6H, $CH_3-C_6H_4-CH(CH_3)_2$), 2.14s (3H, $CH_3-C_6H_4-CH(CH_3)_2$), 2.47s (3H, C5−CH_3 of HL^2), 2.57s (3H, C3−CH_3 of HL^2), 2.92m (1H, $CH_3-C_6H_4-CH(CH_3)_2$), 5.70d, 5.86d (4H, AA′BB′ system, $CH_3-C_6H_4-CH(CH_3)_2$), 6.15s (2H, H_4 of HL^2), 6.55s (C−*H* of HL^2), 7.35mbr, 7.43m (15H, P−C_6H_5), COO*H* of HL^2 not observed. ^{31}P{^{1}H} ($CDCl_3$): δ 4.39s (free *P*Ph$_3$), 30.32s (*O*=*P*Ph$_3$), 35.81s (Ru−*P*Ph$_3$). ^{13}C{^{1}H} ($CDCl_3$): δ 12.84 (sbr, C5−CH_3 of HL^2), 15.44 (sbr, 3-CH_3 of HL^2), 16.62, 19.05 (s, $CH_3-C_6H_4-CH(CH_3)_2$), 23.30, 24.26 (s, CH_3-

$C_6H_4{-}CH(\mathit{C}H_3)_2$), 31.50 (s, $CH_3{-}C_6H_4{-}\mathit{C}H(CH_3)_2$), 66.01, 66.60 (sbr, $\mathit{C}{-}H$ of HL^2), 84.90, 85.72, 102.9, 106.8 (sbr, $CH_3{-}\mathit{C_6}H_4{-}CH(CH_3)_2$), 109.86 (s, C_4 of HL^2), 128.81, 132.39, 134.18 (mbr, $P{-}\mathit{C_6}H_5$) 145.31 (s, C_5 of HL^2), 156.78 (s, C_3 of HL^2), 163.94 (s, *C*OOH of HL^2). ESI-MS (+) H_2O (*m*/*z*, relative intensity %): 483 [100] $[Ru(cymene)(L^2)]^+$, 533 [20] $[Ru(cymene)(PPh_3)Cl]^+$. ESI-MS (+) CH_3CN (*m*/*z*, relative intensity %): 475 [40] $[Ru(cymene)(H_2C(3{,}5\text{-}Me_2pz)_2)Cl]^+$, 519 [30] $[Ru(cymene)(HL^2)Cl]^+$, 533 [100] $[Ru(cymene)(PPh_3)Cl]^+$, 574 [20] $[Ru(cymene)(PPh_3)(CH_3CN)Cl]^+$.

[Ru(η^6-*p*-cymene)(κ^3-*N*,*N′*,*O*-L^1)]Cl (9). [Ru(η^6-*p*-cymene)Cl(μ-Cl)]$_2$ (0.306 g, 0.5 mmol) was dissolved in methanol (20 mL) and stirred 30 min. Then, a methanol solution of HL^1 (0.192 g, 1.0 mmol) and $NaOCH_3$ (0.054 g, 1.0 mmol) was added, and the reaction mixture immediately changed to orange. After 24 h of stirring at room temperature, the clear orange solution was evaporated to dryness and redissolved in chloroform (5 mL) and the salt NaCl removed by filtration. The filtered solution was dried on rotavapor and the solid residue crystallized from methanol. The powder was identified as derivative **9**. It is soluble in DMSO, water, and methanol. Yield: 65%. Mp > 280 °C dec. Anal. calcd for $C_{18}H_{21}ClN_4O_2Ru$: C, 46.80; H, 4.58; N, 12.13. Found: C. 46.35; H, 4.38; N, 12.20%. Λ_m (H_2O, 298 K, 10^{-4} mol/L): 134.73 Ω^{-1} cm^2 mol^{-1}. IR (nujol, cm^{-1}): 3103m $\nu(C_{arom}{-}H)$, 1663s $\nu_{asym}(COO)$, 1508m $\nu(C{=}N + C{=}C)$, 1500w $\nu_{sym}(COO)$. ^1H (D_2O): δ 1.05d (6H, $CH_3{-}C_6H_4{-}CH(C\mathit{H}_3)_2$), 2.12s (3H, $C\mathit{H}_3{-}C_6H_4{-}CH(CH_3)_2$), 2.88m (1H, $CH_3{-}C_6H_4{-}C\mathit{H}(CH_3)_2$), 5.79d, 5.81d (4H, AA′BB′ system, $CH_3{-}C_6\mathit{H}_4{-}CH(CH_3)_2$), 6.54t (2H, H_4 of L^1), 6.92s (C−*H* of L^1), 7.93d (2H, H_5 of L^1), 8.56d (2H, H_3 of L^1). $^{13}C\{^1H\}$ (D_2O): δ 14.91 (s, $\mathit{C}H_3{-}C_6H_4{-}CH(CH_3)_2$), 19.12 (s, $CH_3{-}C_6H_4{-}CH(\mathit{C}H_3)_2$), 28.14 (s, $CH_3{-}C_6H_4{-}\mathit{C}H(CH_3)_2$), 69.05 (s, *C*−H of L^1), 83.52, 80.46, 100.10, 101.25 (s, $CH_3{-}\mathit{C_6}H_4{-}CH(CH_3)_2$), 106.77 (s, C_4 of L^1), 131.75 (s, C_5 of L^1), 144.33 (s, C_3 of L^1), 165.11 (s, *C*OO of L^1). ESI-MS (+) H_2O (*m*/*z*, relative intensity %): 427 [100] $[Ru(cymene)(L^1)]^+$.

[Ru(η^6-*p*-cymene)(κ^3-*N*,*N′*,*O*-L^1)]PF_6 (10). Derivative **1** (0.498 g, 1.0 mmol) was dissolved in methanol (20 mL); then, NaOMe (0.054 g, 1.0 mmol) and NH_4PF_6 (0.163 g, 1.0 mmol) were added to the solution and stirred for 2 h at room temperature. Slow evaporation afforded a crystalline solid identified as derivative **10**. It is very soluble in water, methanol, and acetonitrile. Yield: 92%. Mp 265−269 °C. Anal. calcd for $C_{18}H_{21}F_6N_4O_2PRu$: C, 37.83; H, 3.70; N, 9.80. Found: C. 37.67; H, 3.65; N, 9.63%. Λ_m (acetonitrile, 298 K, 10^{-4} mol/L): 122 Ω^{-1} cm^2 mol^{-1}. Λ_m (H_2O, 298 K, 10^{-4} mol/L): 134 Ω^{-1} cm^2 mol^{-1}. IR (nujol, cm^{-1}): 3146m $\nu(C_{arom}{-}H)$, 1671s $\nu_{asym}(COO)$, 1508m $\nu(C{=}N + C{=}C)$, 833vs, 556s $\nu(PF_6)$, 287s $\nu(Ru{-}Cl)$. ^1H (D_2O): δ 1.05d (6H, $CH_3{-}C_6H_4{-}CH(C\mathit{H}_3)_2$), 2.12s (3H, $C\mathit{H}_3{-}C_6H_4{-}CH(CH_3)_2$), 2.88m (1H, $CH_3{-}C_6H_4{-}C\mathit{H}(CH_3)_2$), 5.79d, 5.81d (4H, AA′BB′ system, $CH_3{-}C_6\mathit{H}_4{-}CH(CH_3)_2$), 6.54t (2H, H_4 of L^1), 7.93d (2H,H_5 of L^1), 8.56d (2H,H_3 of L^1), 6.92s (C−*H* of L^1). $^{13}C\{^1H\}$ (D_2O): δ n. o. (s, $\mathit{C}H_3{-}C_6H_4{-}CH(CH_3)_2$), 24.33 (s, $CH_3{-}C_6H_4{-}CH(\mathit{C}H_3)_2$), n.o. (s, $CH_3{-}C_6H_4{-}\mathit{C}H(CH_3)_2$), *C*−H of L^1 not observed, 85.70, 88.75 (s, AA′BB′ system, $CH_3{-}C_6H_4{-}CH(CH_3)_2$), 112.01 (s, C_4 of L^1), 136.94 (s, C_5 of L^1), 149.56 (s, C_3 of L^1), *C*OO of L^1 not observed. ESI-MS (+) H_2O (*m*/*z*, relative intensity %): 427 [100] $[Ru(cymene)(L^1)]^+$. ESI-MS (+) CH_3CN (*m*/*z*, relative intensity %): 427 [100] $[Ru(cymene)(L^1)]^+$.

[Ru(η^6-benzene)(κ^3-*N*,*N′*,*O*-L^2)]Cl (11). Derivative **11** was prepared following a procedure similar to that reported for **9** by using [Ru(η^6-benzene)Cl(μ-Cl)]$_2$ (0.250 g, 0.5 mmol), HL^2 (0.248 g, 1.0 mmol), and $NaOCH_3$ (0.054 g, 1.0 mmol) in 4:1 acetonitrile/methanol (20 mL). The powder was identified as derivative **5**. It is very soluble in water and chloroform. Yield: 86%. Mp > 270 °C dec. Anal. calcd for $C_{18}H_{21}ClN_4O_2Ru$: C, 46.80; H, 4.58; N 12.13. Found: C, 46.57; H, 4.61; N, 12.16%. Λ_m (H_2O, 298 K, 10^{-4} mol/L): 64 Ω^{-1} cm^2 mol^{-1}. IR (nujol, cm^{-1}): 3131m $\nu(C_{arom}{-}H)$, 1662m $\nu_{asym}(COO)$, 1561m $\nu(C{=}N + C{=}C)$. ^1H (D_2O): δ 2.31s (3H, $C5{-}C\mathit{H}_3$ of L^2), 2.44s (3H, 3-$C\mathit{H}_3$ of L^2), 5.93s (6H, $C_6\mathit{H}_6$), 6.18s (2H, H_4 of L^2), 6.57s (C−*H* of L^2). $^{13}C\{^1H\}$ (D_2O): δ, 13.80 (s, $C5{-}\mathit{C}H_3$ of L^2), 18.12 (s, $C3{-}\mathit{C}H_3$ of L^2), 70.50 (s, *C*−H of L^2), 88.82 (s, $\mathit{C_6}H_6$), 112.16 (s, C_4 of L^2), 148.25 (s, C_5 of L^2), 158.91 (s, C_3 of L^2), 171.44 (s, *C*OO of L^2). ESI-MS (+), H_2O: 472 [100] $[Ru(benzene)(L^2)(HCOOH)]^+$. ESI-MS (+) CH_3CN (*m*/*z*, relative intensity %): 472 [100] $[Ru(benzene)(L^2)(HCOOH)]^+$.

Table 1. Crystal Data and Experimental Details for **10**

compound	**10**
formula	$C_{18}H_{21}F_6N_4O_2PRu$
fw	571.43
T, K	293(2)
λ, Å	0.71073
cryst symmetry	monoclinic
space group	$P2_1/c$
A, Å	10.2845(5)
B, Å	12.6113(6)
C, Å	16.5250(8)
β, deg	90.527(1)
cell volume, Å^3	2143.2(2)
Z	4
D_{calcd}, Mg m^{-3}	1.771
μ(Mo Kα), mm^{-1}	0.881
F(000)	1144
cryst size/ mm	0.30 × 0.25 × 0.10
θ limits, deg	2.03−27.00
reflns collected	17492 ($\pm h$, $\pm k$, $\pm l$)
unique obs. reflns [$F_o > 4\sigma(F_o)$]	4667 [R(int) = 0.0214]
goodness-of-fit-on F^2	1.100
R_1(F),[a] wR_2 (F^2)[b]	0.0379, 0.1065
largest diff. peak and hole, e Å^{-3}	1.016 and −0.755

[a] $R_1 = \sum||F_o| - |F_c|| / \sum|F_o|$. [b] $wR_2 = [\sum w(F_o^2 - F_c^2)^2 / \sum w(F_o^2)^2]^{1/2}$, where $w = 1/[\sigma^2(F_o^2) + (aP)^2 + bP]$, where $P = (F_o^2 + 2F_c^2)/3$.

[Ru(η^6-benzene)(κ^3-*N*,*N′*,*O*-L^2)]PF_6 (12). Derivative **11** (0.462 g, 1.0 mmol) was dissolved in chloroform (20 mL) and stirred for 30 min; then, NH_4PF_6 (0.163 g, 1.0 mmol) was added to the red solution, which immediately changed to orange. After 2 h of stirring at room temperature, the solution was filtered to remove ammonium chloride; the solvent was removed in vacuo and the residue dried under reduced pressure. The powder was identified as derivative **12**. It is very soluble in water, acetonitrile, methanol, and chloroform. Yield: 87%. Mp > 250 °C dec. Anal. calcd for $C_{18}H_{21}F_6N_4O_2PRu$: C. 37.83; H, 3.70; N 9.80. Found: C, 37.78; H, 3.69; N, 9.72%. Λ_m (acetonitrile, 298 K, 10^{-4} mol/L): 27 Ω^{-1} cm^2 mol^{-1}. Λ_m (H_2O, 298 K, 10^{-4} mol/L): 58 Ω^{-1} cm^2 mol^{-1}. IR (nujol, cm^{-1}): 3100m $\nu(C_{arom}{-}H)$, 1661m $\nu_{asym}(COO)$, 1560m $\nu(C{=}N + C{=}C)$, 840m $\nu(PF_6)$. ^1H (D_2O): δ 2.28s (3H, 5-$C\mathit{H}_3$ of L^2), 2.38s (3H, 3-$C\mathit{H}_3$ of L^2), 5.84s (6H, $C_6\mathit{H}_6$), 6.10s (2H, H_4 of L^2), 6.51s (C−*H* of L^2). ^1H ($CDCl_3$): δ 2.49s (3H, 5-$C\mathit{H}_3$ of L^2), 2.71s (3H, 3-$C\mathit{H}_3$ of L^2), 6.07s (6H, $C_6\mathit{H}_6$), 6.21s (2H, H_4 of L^2), 7.27s (C−*H* of L^2). $^{31}P\{^1H\}$($CDCl_3$): δ −156.50, −152.11, −147.71, −143.32, −138.93, −134.53, −130.13. $^{13}C\{^1H\}$ ($CDCl_3$): δ 12.13 (s, $\mathit{C}5{-}\mathit{C}H_3$ of L^2), 15.8 (s, $\mathit{C}3{-}\mathit{C}H_3$ of L^2), 77.25 (s, *C*−H of L^2), 82.39 (s, $\mathit{C_6}H_6$), 109 (s, C_4 of L^2), 142.21 (s, C_5 of L^2), 155.98 (s, C_3 of L^2), 170 (s, *C*OO of L^2). ESI-MS (+) H_2O (*m*/*z*, relative intensity %): 427 [10] $[Ru(benzene)(L^2)]^+$, 472 [100] $[Ru(benzene)(L^2)(HCOOH)]^+$, 844 [10] $[\{Ru(benzene)(OH)\}_2(L^2)(H_2C(3{,}5\text{-}Me_2pz)_2)]^+$.

X-Ray Crystallography for 10. The X-ray intensity data for **10** were measured on a Bruker SMART Apex II CCD area detector diffractometer. Cell dimensions and the orientation matrix were initially determined from a least-squares refinement on reflections measured in three sets of 20 exposures, collected in three different ω regions, and eventually refined against all data. A full sphere of reciprocal space was scanned by 0.3° ω steps. The software SMART[19] was used for collecting frames of data,

---

(19) *SMART & SAINT Software Reference Manuals*, version 5.051 (Windows NT Version); Bruker Analytical X-ray Instruments Inc.: Madison, WI, 1998.

Scheme 1

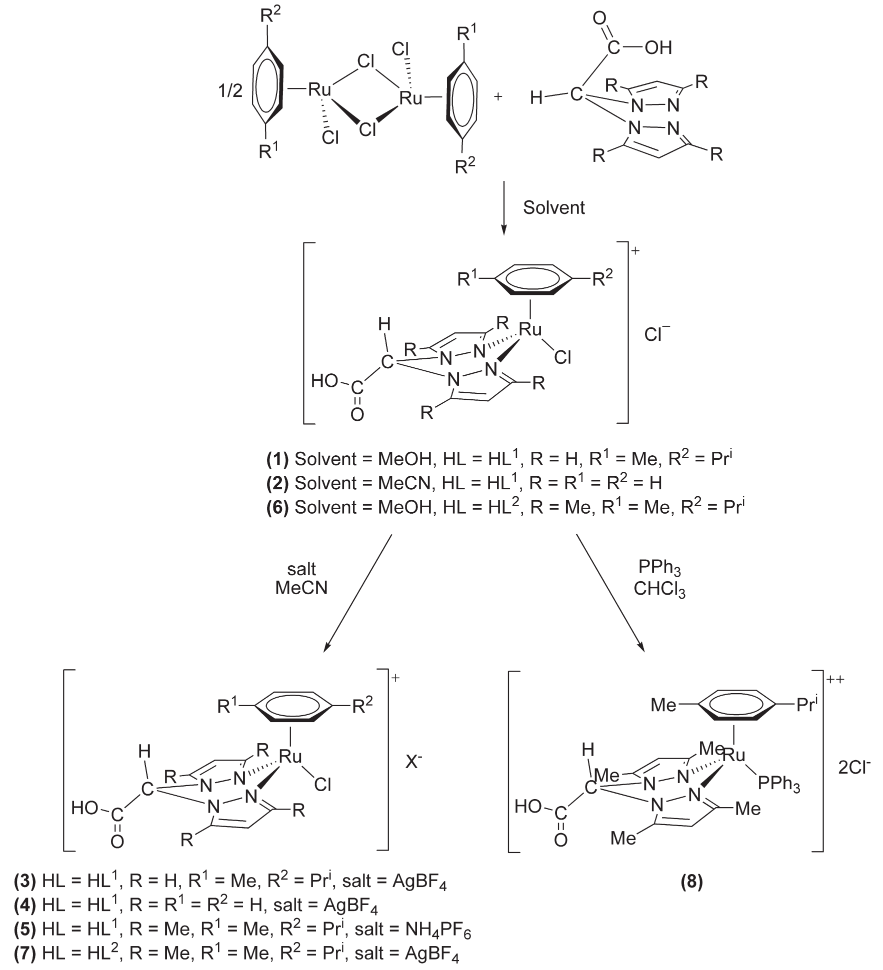

(1) Solvent = MeOH, HL = HL^1, R = H, R^1 = Me, R^2 = Pr^i
(2) Solvent = MeCN, HL = HL^1, R = R^1 = R^2 = H
(6) Solvent = MeOH, HL = HL^2, R = Me, R^1 = Me, R^2 = Pr^i

(3) HL = HL^1, R = H, R^1 = Me, R^2 = Pr^i, salt = $AgBF_4$
(4) HL = HL^1, R = R^1 = R^2 = H, salt = $AgBF_4$
(5) HL = HL^1, R = Me, R^1 = Me, R^2 = Pr^i, salt = NH_4PF_6
(7) HL = HL^2, R = Me, R^1 = Me, R^2 = Pr^i, salt = $AgBF_4$

(8)

indexing reflections, and determination of lattice parameters. The collected frames were then processed for integration by the SAINT program,[19] and an empirical absorption correction was applied using SADABS.[20] The structure was solved by direct methods (SIR 97)[21] and subsequent Fourier syntheses and refined by full-matrix least-squares on F^2 (SHELXTL),[22] using anisotropic thermal parameters for all non-hydrogen atoms. The PF_6^- anion was found disordered over two orientations, yielding two distinct F_6 octahedra around the P center (0.62 and 0.38 occupation factors, respectively). All hydrogen atoms were added in calculated positions, included in the final stage of refinement with isotropic thermal parameters, $U(H) = 1.2\ U_{eq}(C)$ [$U(H) = 1.5\ U_{eq}(C{-}Me)$], and allowed to ride on their carrier carbons. Crystal data and details of the data collection for all structures are reported in Table 1.

Results and Discussion

Synthesis and Spectroscopic Characterization. The direct interaction between dinuclear [Ru(η^6-arene)Cl(μ-Cl)]$_2$ (arene = *p*-cymene or benzene) and HL^1 in methanol or acetonitrile afforded derivatives **1** and **2** (Scheme 1) as air-stable orange solids that are very soluble in alcohols, DMSO, chlorinated solvents, and water. Chloride exchange with bulky anions was carried out through metathesis reactions with $AgBF_4$ or NH_4PF_6 salts that afforded derivatives **3**−**5** (Scheme 1). Similarly, by using HL^2, derivatives **6** and **7** were synthesized (Scheme 1). By the interaction of **6** with equivalent amounts of PPh_3, derivative **8** was obtained (Scheme 1).

Conductivity values of **1**−**8** were investigated in water and, for **3**−**5** and **7** and **8**, also in acetonitrile (derivatives **1**, **2**, and **6** showed only limited solubility in this solvent). While the Λ_M value of **8** in water of 191 Ω^{-1} cm^2 mol^{-1} is typical of 1:2 electrolytes,[23] as expected from its composition, the Λ_M values of derivatives **1**−**7** were in the range 260−380 Ω^{-1} cm^2 mol^{-1}, much higher than typical values of 1:1 electrolytes.[23] Such unexpected results could however be explained by the occurrence of −COOH deprotonation in the HL ligands and consequent formation of species such as [Ru(η^6-arene)(κ^3-*N*,*N*′,*O*-L)](Cl^-,X^-) (where X = Cl, BF_4, or PF_6), together with H_3O^+, which greatly contributes to enhancement of the conductivity values of the solutions (Scheme 2). To further confirm this hypothesis, we have measured the pH values of aqueous solutions of **1** and **2** at different concentrations. Our measurements have been carried out in the range 10^{-2} to 10^{-4} molar. The pH values found are in the range 2.5−4.5, in accordance with a relevant deprotonation of the

---

(20) Sheldrick, G. M. *SADABS*; University of Göttingen: Göttingen, Germany, 1996.

(21) Altomare, A.; Burla, M. C.; Camalli, M.; Cascarano, G. L.; Giacovazzo, C.; Guagliardi, A.; Moliterni, A. G. G.; Polidori, G., Spagna, R. *J. Appl. Crystallogr.* **1999**, *32*, 115.

(22) Sheldrick, G. M. *SHELXTLplus*, version 5.1 (Windows NT version); Bruker Analytical X-ray Instruments Inc.: Madison, WI, 1998.

(23) Geary, W. J. *Coord. Chem. Rev.* **1971**, *7*, 81.

Scheme 2

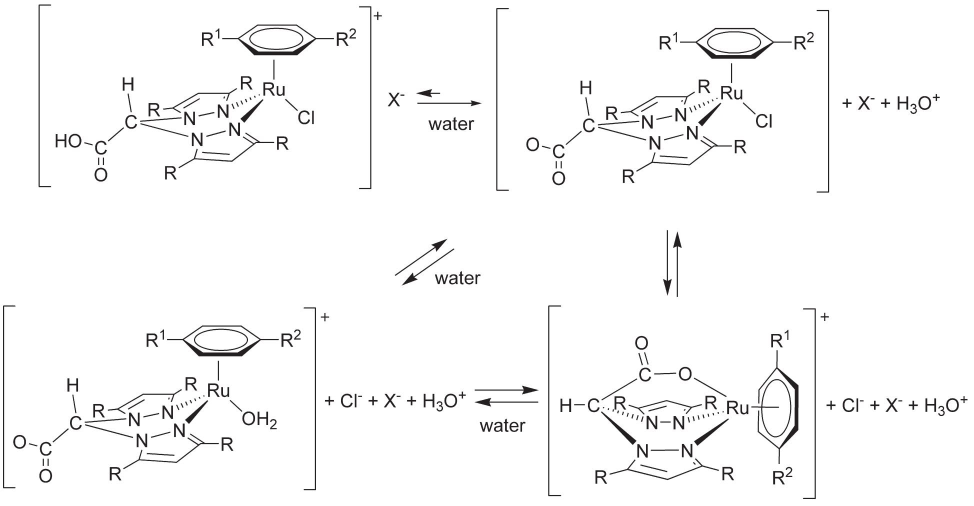

ligand in the cationic complexes. However, a determination of the K_a values under these conditions has not been performed due to the likely existence of different equilibria among species formed in solution, such as those shown in Scheme 2.

The relatively lower Λ_M values of **6** and **7**, with respect to those of **1**−**5**, are clearly ascribed to their different structures, that is, to the presence of methyl substituents in pyrazoles of the HL^2 ligand. The electron density donation from HL^2 to Ru is stronger than in the case of the HL^1 ligand and reduces the attraction of Ru for the oxygen of −COOH. This, in turn, reduces the tendency toward deprotonation and hence shifts the position of the equilibrium for **6** and **7** to the left with respect to that of **1**−**5**. Additionally, in compound **8**, the presence also of the bulky and weakly basic PPh_3 ligand in the metal coordination sphere seems to hamper the tridentate coordination of the bis(pyrazolyl)acetate ligand, and a normal Λ_M value has been observed. The Λ_M values in acetonitrile solutions of **3**−**5**, **7**, and **8** are in the range reported for 1:1 electrolytes,[23] thus indicating that the previous equilibrium is not operating in this solvent, or at least it is less shifted to the right than in water.

When the interaction between [Ru(η^6-*p*-cymene)Cl(μ-Cl)]$_2$ and HL^1 was carried out in methanol in the presence of sodium methoxide, derivative **9** was isolated, which exchanges external chloride with PF_6^- by interaction with NH_4PF_6 in acetonitrile, affording **10** (Scheme 3). Similarly, from [Ru(η^6-benzene)Cl(μ-Cl)]$_2$ and HL^2 in acetonitrile in the presence of sodium methoxide, derivative **11** was obtained, which reacts with NH_4PF_6 in chloroform, affording **12** (Scheme 3). Conductivity values in water of **9**−**12** are in accordance with those of 1:1 electrolytes.[23]

The ESI-MS spectra of **1**−**8** carried out in water confirm our previous hypothesized extensive deprotonation in aqueous solution of metal-bound HL^1 and HL^2. In fact, the spectra of **1**, **3**, and **5** display only a peak at 427 *m*/*z* (Figure 2S, Supporting Information) due to the [Ru(cymene)(L^1)]$^+$ fragment, arising from the deprotonation of HL^1 and the expulsion of the chloride from the metal coordination sphere. Of course, the spectra of derivatives **9** and **10** are also coincident with the previous ones. Similarly, the spectra of **2** and **4** show a single peak at 371 *m*/*z* (Figure 3S, Supporting Information), assignable to the [Ru(benzene)(L^1)]$^+$ fragment.

Scheme 3

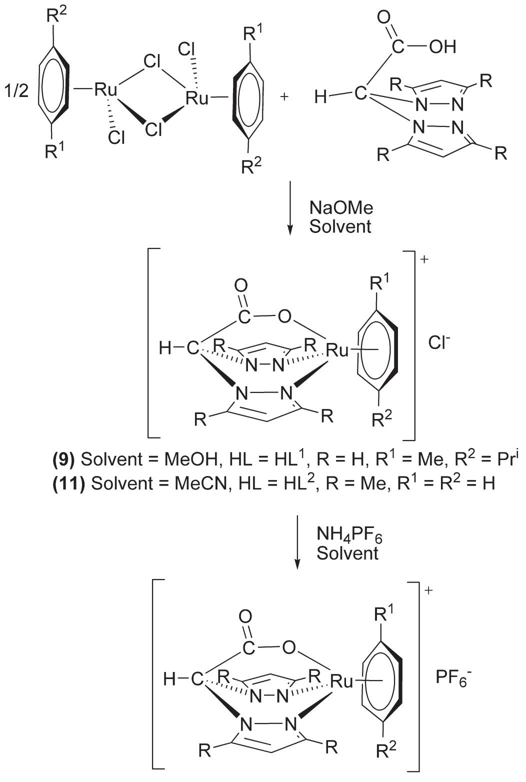

(**9**) Solvent = MeOH, HL = HL^1, R = H, R^1 = Me, R^2 = Pr^i
(**11**) Solvent = MeCN, HL = HL^2, R = Me, R^1 = R^2 = H

(**10**) Solvent = MeOH, HL = HL^1, R = H, R^1 = Me, R^2 = Pr^i
(**12**) Solvent = $CHCl_3$, HL = HL^2, R = Me, R^1 = R^2 = H

In the ESI-MS spectra of HL^2-containing derivatives **6** and **7**, two peaks have been found, the most intense at 483 *m*/*z* being due to [Ru(cymene)(L^2)]$^+$, while the small peak at 519 *m*/*z* can be assigned to [Ru(cymene)(HL^2)(Cl)]$^+$, in agreement with the lower tendency toward deprotonation of coordinated HL^2. However, the ESI-MS spectrum of derivative **8** shows a peak at 483 *m*/*z* due to [Ru(cymene)(L^2)]$^+$ and another one at 533 *m*/*z* due to [Ru(cymene)(PPh_3)Cl]$^+$.

The peak at 427 *m*/*z* for derivatives **11** and **12** is due to [Ru(benzene)(L^2)]$^+$; moreover, two additional peaks have been found in the spectrum of **12**, one at 472 *m*/*z* assigned to [Ru(benzene)(L^2)(HCOOH)]$^+$ (HCOOH = formic acid) and another at 844 *m*/*z* assigned to the dinuclear fragment [{Ru(benzene)(OH)}$_2$(L^2)(H_2C(3,5-$Me_2pz)_2$)]$^+$ (H_2C(3,5-$Me_2pz)_2$ = bis(3,5-dimethylpyrazol-1-yl)methane), where the formic acid and the N_2-chelating ligand H_2C(3,5-$Me_2pz)_2$[10] arise from decarboxylation of the L^2 ligand.

The ESI-MS spectra of **2**–**5** recorded in MeCN are unexpectedly essentially similar to those in water, and the discrepancy with the conductivity values in MeCN can be ascribed to different, more drastic conditions associated with the ESI-MS spectrometry. For derivatives **6**–**8**, a number of additional peaks have been observed, such as that at 475 *m*/*z* due to [Ru(cymene)(H_2C(3,5-$Me_2pz)_2$)-Cl]$^+$, arising from decarboxylation of the L^2 moiety, and that in the spectrum of **8** at 574 *m*/*z* due to [Ru(cymene)-(PPh_3)(MeCN)Cl]$^+$.

The solid-state IR spectra of **1**–**8** clearly show that carboxylic groups in HL^1 and HL^2 are uncoordinated, as the absorptions of –COOH fall in the range 1700–1770 cm^{-1}, being practically unaffected or only slightly shifted with respect to those found in the IR spectra of free ligands.[6] Also, the broad bands over 3300 cm^{-1} have always been detected, likely due to the –COO–H group of the HL ligand being involved in H bonding with another –COO–H of a vicinal complex ion or with the anion Cl^-, BF_4^-, or PF_6^-. In fact, the IR spectra of derivatives **3**–**5** and **7** show the typical absorptions of ionic BF_4[24] or PF_6 anions,[25] even if the presence of some fine splitting could be ascribed to the previously hypothesized H-bonding interaction X–F···H–O (X = B or P) involving the COOH of HL ligands that likely occurs in the solid state. Moreover, in the far-IR region, a strong absorption due to Ru–Cl has always been observed, in accordance with the coordination of ligands HL^1 and HL^2 in their neutral *N*,*N*′-bidentate form. In the far-IR of **8**, the typical absorptions due to *y*- and *t*-stretching modes (Whiffen notation) of triphenylphosphine have also been detected.[26]

On the contrary, in the IR spectra of **9**–**12**, the carboxylic bands of deprotonated L ligands were found in the range 1660–1675 cm^{-1}, that is, shifted to a lower frequency with respect to free neutral HL, thus indicating the coordination of L in a N,N,O-tridentate tripodal form.[6] Accordingly, no Ru–Cl absorption band has been observed in the far-IR region. Moreover, in **10** and **12**, the typical pattern of ionic PF_6 has been detected,[23] and an X-ray diffraction study has been carried out on **10** (see later).

The ^{1}H, ^{13}C, ^{19}F, and ^{31}P NMR spectra were recorded in D_2O and also in $CDCl_3$ and CD_3CN. It is interesting to note the coincidence of proton spectra in D_2O of derivatives **1**, **3**, and **5** with those of compounds **9** and **10**, as the consequence of the deprotonation of HL^1 in water. Moreover, ^{1}H NMR spectra in D_2O of **2** and **4** are overlapping. Similarly, those of **6** and **7** are practically the same, as well as those of **11** and **12**. When $CDCl_3$ or CD_3CN are employed as solvents, the proton spectra of derivatives containing neutral pyrazolylacetate ligands generally show resonances due to the –COOH fragment, in accordance with the existence in these solvents of the (arene)Ru(II) adducts with neutral *N*,*N*-bidentate HL^1 and HL^2 ligands. The ^{1}H NMR spectrum in $CDCl_3$ of compound **8** shows the phosphino resonances with the correct integration with respect to those of cymene and of the HL^2 ligand. Its ^{31}P NMR spectrum contains a resonance at 35.8 ppm due to the Ru-bound PPh_3, together with a small resonance at 4.4 ppm due to free phosphine and an additional small peak at 30.3 ppm likely caused by oxidized *O*=PPh_3. Hence, in the chloroform solution, a dissociation equilibrium of phosphine is operating at room temperature.

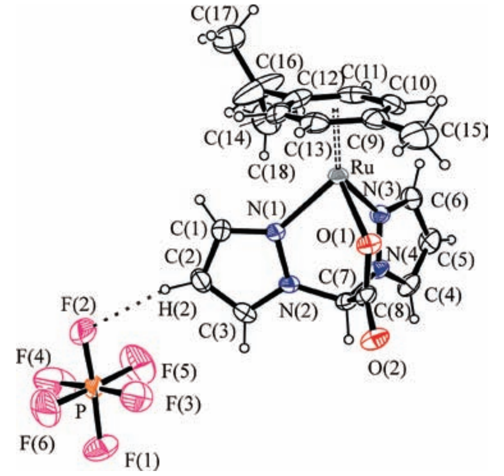

Figure 1. ORTEP drawing of **10**. Dotted lines indicate the weak F(2)···H(2)–C(2) interaction. Thermal ellipsoids are drawn at the 30% probability level.

Table 2. Selected Bond Lengths (Å) and Angles (deg) for **10**

Ru(1)–N(1)	2.097(3)	Ru(1)–C(12)	2.206(4)
Ru(1)–N(3)	2.098(3)	Ru(1)–C(13)	2.158(4)
Ru(1)–O(1)	2.093(2)	Ru(1)–C(14)	2.165(4)
Ru(1)–C(9)	2.190(4)	Ru(1)–Ct(centroid)	1.669
Ru(1)–C(10)	2.176(3)	O(1)–C(8)	1.278(4)
Ru(1)–C(11)	2.169(4)	O(2)–C(8)	1.214(4)
N(3)–Ru(1)–N(1)	84.1(1)	C(7)–C(8)–O(1)	115.7(3)
N(3)–Ru(1)–O(1)	83.6(1)	C(8)–C(7)–N(2)	108.8(2)
N(1)–Ru(1)–O(1)	82.4(1)	C(8)–C(7)–N(4)	111.7(3)

X-Ray Diffraction Studies of 10. The crystal structure of the cation of **10** is shown in Figure 1, and relevant bond lengths and angles are reported in Table 2. In complex **10**, the cation adopts the expected three-legged piano stool structure, that being the ruthenium atom η^6-bonded to the *p*-cymene ring and k^3-coordinated by the bpza [bis(pyrazol-1-yl)acetate] ligand. The Ru–C(*p*-cymene) average bond length of 2.177 Å [range 2.158–2.206(4) Å] is shorter than those found in similar complexes, [(*p*-cymene)Ru{$H_2C(pz)_2$}Cl]Cl, [(*p*-cymene)Ru($H_2C\{pz^{4Me}\}_2$)-Cl]Cl, and [(*p*-cymene)Ru{$H_2C(pz)_2$}Cl](O_3SCF_3)] (2.194, 2.193, and 2.194 Å, respectively).[10] The heteroscorpionate

---

[24] Rosenthal, M. R. *J. Chem. Educ.* **1973**, *50*, 331.

[25] (a) Kruck, T. *Angew. Chem., Int. Ed.* **1967**, *6*, 53. (b) Collong, W.; Kruck, T. *Chem. Ber.* **1990**, *123*, 1655. (c) Fuss, W.; Ruhe, M. *Z. Naturforsch.* **1992**, *47B*, 1.

[26] (a) Bradbury, J.; Forest, K. P.; Nuttall, R. H.; Sharp, D. W. A. *Spectrochim. Acta* **1967**, *23*, 2701. (b) Green, J. H. S. *Spectrochim. Acta* **1968**, *24A*, 137. (c) Shobatake, K.; Postmus, C.; Ferraro, J. R.; Nakamoto, K. *Appl. Spectrosc.* **1969**, *23*, 12. (d) Clark, R. J. H.; Flint, C. D.; Hempleman, A. J. *Spectrochim. Acta* **1987**, *42A*, 805.

Table 3. Cyclic Voltammetric Data and the Calculated Vertical Ionization Potential (I_v) and HOMO Energy (E_{HOMO}) for Arene-Ru(II) Derivatives with Bis(pyrazol-1-yl) acetate and 4-Acyl-5-pyrazolonato Ligands[a]

no.	compound	$E_{1/2}^{ox\,b}$/V vs SCE	$E_{1/2}^{ox}$/V vs NHE	I_v/eV	E_{HOMO}/eV[c]
2	$[Ru(\eta^6\text{-benzene})(HL^1)Cl]Cl$	(+1.76)	(+2.01)		
3	$[Ru(\eta^6\text{-}p\text{-cymene})(HL^1)Cl]BF_4$	+1.72	+1.97		
4	$[Ru(\eta^6\text{-benzene})(HL^1)Cl]BF_4$	(+1.71)	(+1.96)	10.90	−9.31
5	$[Ru(\eta^6\text{-}p\text{-cymene})(HL^1)Cl]PF_6$	+1.69	+1.94		
6	$[Ru(\eta^6\text{-}p\text{-cymene})(HL^2)Cl]Cl$	(+1.58)	(+1.83)		
7	$[Ru(\eta^6\text{-}p\text{-cymene})(HL^2)Cl]BF_4$	+1.64	+1.89	10.66[d]	−9.23[d]
8	$[Ru(\eta^6\text{-}p\text{-cymene})(HL^2)(PPh_3)]Cl_2$[e]	(+2.04)	(+2.29)		
10	$[Ru(\eta^6\text{-}p\text{-cymene})(L^1)]PF_6$	(+1.78)	(+2.03)	11.22[d]	−9.73[d]
11	$[Ru(\eta^6\text{-benzene})(L^2)]Cl$	(+1.64)	(+1.89)		
12	$[Ru(\eta^6\text{-benzene})(L^2)]PF_6$	+1.61	+1.86	10.70	−9.31
13	$[Ru(\eta^6\text{-}p\text{-cymene})Cl_2(PPh_3)]$[f]	+1.14	+1.39	7.19	−5.61
14	$[Ru(\eta^6\text{-benzene})Cl_2(PPh_3)]$[f]	+1.25	+1.50	7.41	−5.75
15	$[Ru(\eta^6\text{-}p\text{-cymene})(Q^{nPe})Cl]$[f]	+1.30[g]	+1.55	6.89[d,g,h]	−5.49[d,h]
16	$[Ru(\eta^6\text{-}p\text{-cymene})(Q^{naph})Cl]$[f]	+1.38[g]	+1.63	6.79[d,i]	−5.47[d,i]
17	$[Ru(\eta^6\text{-}p\text{-cymene})(Q^{Me,nPe})Cl]$[f]	+1.25[g]	+1.50	6.95[d,j]	−5.42[d,j]
18	$[Ru(\eta^6\text{-}p\text{-cymene})(Q^{CF_3})Cl]$[f]	+1.57[g]	+1.82	7.18[d,k]	−5.80[d,k]

[a] The oxidation potentials of the complexes were measured by CV ($\nu = 1.5\ V\ s^{-1}$), in the presence of ferrocene as the internal standard, and the redox potential values are quoted relative to the SCE by using the $[Fe(\eta^5\text{-}C_5H_5)_2]^{0/+}$ ($E_{1/2}^{ox} = 0.450$ V vs SCE) redox couple in a 0.2 M $CH_3CN/[Bu_4N][BF_4]$ solution. The values relative to the NHE were obtained by adding 0.245 V to those relative to the SCE; compounds **1** and **9** could not be studied due to their insufficient solubility in common electrochemical solvents (i.e., CH_3CN, CH_2Cl_2, or THF). [b] Half-wave oxidation potential of a reversible or quasi-reversible oxidation wave. For the irreversible waves, $E_{p/2}^{ox}$ is given in brackets; for all of the compounds with Cl^- as the counterion, the irreversible oxidation wave of Cl^- is observed at $E_{p/2}^{ox}$ = ca. 1.20 V. Usually, two irreversible reduction waves are also observed, at E_p^{red} in the ca. −0.9 to −1.4 V and −1.5 to −1.8 V ranges, assigned to the reductions of the ligands. [c] In the case of the anionic complexes, the counterion was not included in the calculations. [d] For benzene derivatives (complexes **7'**, **10'**, **15'**−**18'**). [e] An oxidation wave at $E_{1/2}^{ox} = +1.68$ V is assigned to $[Ru(\eta^6\text{-}p\text{-cymene})(HL^2)(Cl)]^+$ (see **7**) derived from the partial PPh_3 ligand replacement by Cl^-, in the electrolyte solution. [f] Included for comparison (see text and Table 4). [g] Ref 7. [h] For Q^{nPe} = 1-phenyl-4-acetyl-5-pyrazolonate (**15'**). [i] For Q^{naph} = 1-phenyl-4-benzoyl-5-pyrazolonate (**16'**). [j] For $Q^{Me,nPe}$ = 1-methyl-4-acetyl-5-pyrazolonate (**17'**). [k] For Q^{CF_3} = 1-phenyl-4-trifluoroacetyl-5-pyrazolonate (**18'**).

bpza ligand coordinates to the Ru atom with one carboxylate oxygen [Ru(1)−O(1) 2.093(2) Å] and two N atoms [Ru(1)−N(1), 2.097; Ru(1)−N(3), 2.098(2) Å]. The angles at the Ru atom of the N,N,O tripodal ligand are very close to each other [N(1)−Ru(1)−N(3), N(1)−Ru(1)−O(1), and N(2)−Ru(1)−O(1): 84.1, 82.4, and 83.6(1)°, respectively]. Short interionic interactions are present between one fluorine [F(2)] of the PF_6^- anion and one pyrazolyl hydrogen [C(2)···F(2), 3.32(1) Å; H(2)···F(2), 2.41 Å; C(2)−H(2)···F(2), 166°] of the cation.

Electrochemical Studies. The redox properties of the compounds have been investigated by cyclic voltammetry, at a Pt disk electrode, in a 0.2 M $[^nBu_4N][BF_4]/CH_3CN$ solution, at 25 °C. They exhibit a single-electron (reversible, quasi-reversible, or irreversible) oxidation wave that is assigned[27−30] to the $Ru^{II} \rightarrow Ru^{III}$ oxidation, at the half-wave (or half-peak for an irreversible wave) oxidation potential values ($E_{1/2}^{ox}$ or $E_{p/2}^{red}$, respectively) given in Table 3.

The CPE at a potential slightly anodic to that of the $Ru^{II/III}$ peak potential reveals a two-electron oxidation per Ru^{II} atom. The corresponding $Ru^{III/II}$ reduction wave is not observed at the end of the electrolysis, while other reduction waves at different potentials are then detected. This behavior indicates that the oxidized Ru^{III} compound is not stable and is involved in an electrode process with further chemical and electron-transfer reactions. The low stability of the oxidized Ru^{III} complexes is also detected on the shorter time scale of cyclic voltammetry, as shown by Figure 2 in the case of compound **3**. Scan reversal following the $Ru^{II/III}$ oxidation shows the corresponding $Ru^{III/II}$ reduction wave with a lower current intensity and the appearance of another reduction wave at E_p^{red} = 1.19 V versus SCE.

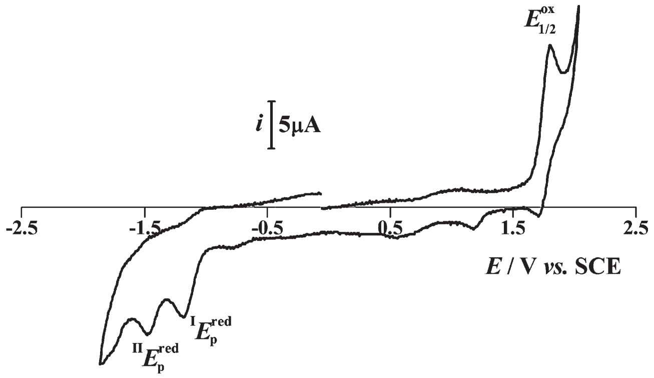

Figure 2. Cyclic voltammogram ($\nu = 1.5\ V\ s^{-1}$) of a 3.0 mM solution of $[Ru(\eta^6\text{-}p\text{-cymene})(HL^1)Cl]BF_4$, **3**, in acetonitrile with 0.2 M $[Bu_4N][BF_4]$, with a platinum disk electrode (d = 0.5 mm).

For the compounds with Cl^- as the counterion, an irreversible oxidation wave is observed at an E_p^{ox} of ca. 1.20 V versus SCE that is assigned to the oxidation of Cl^-. Since the oxidation wave of such compounds is irreversible, in contrast to the others (with a BF_4^- or PF_6^- counterion, which usually displays a reversible oxidation wave), the irreversibility may be due to a nucleophilic attack of Cl^- (or derived chlorine atom) at the Ru^{III} complex formed upon oxidation of the corresponding Ru^{II} compound.

---

(27) (a) Lever, A. B. P. *Inorg. Chem.* **1990**, *29*, 1271. (b) Lever, A. B. P. In *Comprehensive Coordination Chemistry II*; Lever, A. B. P., Ed.; Elsevier: Oxford, 2004; Vol. *2*, Ch. 2.19, pp 251−268 and references therein.

(28) Pombeiro, A. J. L. In *Encyclopedia of Electrochemistry*; Scholz, F., Pickett, C. J., Eds.; Wiley-VCH: New York, 2006; Vol. 7A, Ch. 6, pp 77−108 and references therein.

(29) Reisner, E.; Arion, V. B.; Eichinger, A.; Kandler, N.; Geister, G.; Pombeiro, A. J. L.; Keppler, B. K. *Inorg. Chem.* **2005**, *44*, 6704 and references therein.

(30) Reisner, E.; Arion, V. B.; Guedes da Silva, M. F. C.; Lichteneker, R.; Eichinger, A.; Keppler, B. K.; Kukushkin, V. Yu.; Pombeiro, A. J. L. *Inorg. Chem.* **2004**, *43*, 7083.

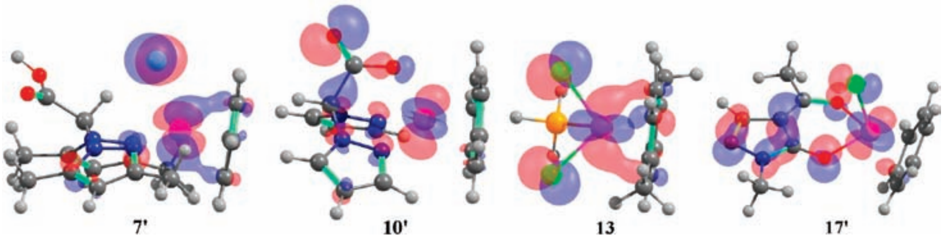

Figure 3. Plots of the HOMO for some of the calculated complexes.

The insolubility of compounds **1** and **9** in the common electrochemical solvents (e.g., MeCN, CH_2Cl_2, or THF) precluded the investigation of their electrochemical behavior. The study in DMSO did not allow detection of the $Ru^{II} \rightarrow Ru^{III}$ oxidation wave at a potential below that of the solvent/electrolyte discharge.

The solution of compound $[Ru(\eta^6\text{-}p\text{-cymene})(HL^2)(PPh_3)]Cl_2$ **8** displays an extra reversible oxidation wave at an $E_{1/2}^{ox}$ value, +1.68 V, that is identical to that of compound **7**, with a chloride ligand instead of PPh_3. The genuine oxidation of **8** is detected at a much higher potential ($E_{p/2}^{red}$ = 2.04 V vs SCE), as expected on account of the higher positive charge of the complex and of the much weaker electron-donor character of the ligated PPh_3 in comparison with Cl^-. The former wave (at +1.68 V) is conceivably due to the oxidation of $[Ru(\eta^6\text{-}p\text{-cymene})(HL^2)Cl]^+$ **7** formed in the electrolyte medium, upon partial replacement of PPh_3 in **8** by the Cl^- counterion.

The η^6-cymene complexes display oxidation potential values that are slightly lower than those of the corresponding η^6-benzene ones [compare, e.g., **5** (1.69 V) with **2** (1.76 V) or **3** (1.72 V) with **2** (1.76 V)], in agreement with the effect, in the former ligand, of the electron-donor substituents. This has been confirmed by measuring the oxidation potential of the related complexes $[Ru(\eta^6\text{-}p\text{-cymene})Cl_2(PPh_3)]$ (**13**) and $[Ru(\eta^6\text{-benzene})Cl_2(PPh_3)]$ (**14**) ($E_{1/2}^{ox}$ = 1.14 and 1.25 V vs SCE, respectively; Table 3), for comparative purposes, and by DFT calculations (see below). Moreover, as expected, these oxidation potential values (for **13** and **14**) are much lower than those of all of the other complexes, on account of the effect of *two* strong electron-donor chloride ligands in the former (**13** and **14**).

The compounds that differ only in the counterion (Cl^- vs BF_4^- or PF_6^-) have similar oxidation potentials, as expected (the small differences arise from the irreversibility of the oxidation process of those with Cl^- as the counterion).

The complexes also show two irreversible reduction waves in the −0.9 to −1.8 V versus SCE range, which involve the bis(pyrazol-1-yl)acetate ligands (when uncoordinated, they undergo irreversible reductions in that range of potential, e.g, at −0.8 and −1.3 V for HL^1 and −0.8 and −1.1 V for HL^2), and were not investigated further.

Computational DFT Studies. In order to rationalize the electrochemical results described above, quantum-chemical calculations of the electronic structure of some of the studied complexes (see Table 3 and the corresponding footnotes) and, for comparative purposes, of the related 4-acyl-5-pyrazolonate Ru^{II} complexes $[Ru(\eta^6\text{-benzene})(Q)Cl]$ (**15′**−**18′**) we have partially reported earlier[31] have been performed at the DFT level of theory.

The calculated structural parameters of $[Ru(\eta^6\text{-benzene})(L^1)]^+$ (**10′**) are in very good agreement with the experimental data for complex **10**. The maximum deviation was found for the $Ru-C_{benzene}$ bonds (0.05 Å) and does not exceed 0.029 Å for the other bonds often lying within the 3σ interval of the experimental data. The analysis of the frontier MO composition of the nonoxidized complexes and the oxidized species with unrelaxed geometry indicates the following features: (*i*) upon oxidation, the electron is removed from the first highest occupied molecular orbital (HOMO) for all calculated complexes. (*ii*) The first HOMO of the bis(pyrazol-1-yl) acetate complexes with the chloride ligand in the inner coordination sphere (i.e., **7′** and **4**) as well as of complexes **13** and **14** is formed mainly by orbitals of the metal and chlorine atoms, whereas the overall contribution from orbitals of the pyrazolylacetate ligand is small (10−15%; Figure 3 and Figure 1S, Supporting Information). (*iii*) In contrast, for the complexes with the tridentate pyrazolylacetate ligand (**12** and **10′**), the involvement of orbitals of this ligand (apart from those of the metal) in the HOMO is significant (mainly from the oxygen atoms). (*iv*) The HOMO of the acylpyrazolonate chloro complexes **15′**−**18′** is also composed by orbitals of the metal and the organic ligand, while the contribution from the Cl atom is insignificant (up to 9%). (*v*) The calculated HOMO energies (E_{HOMO}) and vertical ionization potentials (I_v)[32] generally correlate well (Table 3) with the experimental oxidation potentials, reproducing main trends, for example, higher potentials (lower E_{HOMO}) for the benzene complex **14** in comparison with the cymene species **13** and for the bis(pyrazol-1-yl)acetate complexes **4**, **5**, **7**, **10**, and **12** compared to the acylpyrazolonate species **15**−**18**.

Estimate of the E_L Lever Electrochemical Ligand Parameter. The parametrization of the redox potential of coordination compounds toward the quantification of electronic properties of ligands and binding metal centers is a subject of current attention.[27−30,33,34] In particular the electrochemical Lever E_L ligand parameter[27] constitutes a measure of the electron donor character of a ligand (the

---

(31) Marchetti, F.; Pettinari, C.; Pettinari, R.; Cerquetella, A.; Cingolani, A.; Chan, E. J.; Kozawa, K.; Skelton, B. W.; White, A. H.; Wanke, R.; Kuznetsov, M. L.; Martins, L. M. D. R. S.; Pombeiro, A. J. L. *Inorg. Chem.* **2007**, *46*, 8245.

(32) Vertical ionization potentials are calculated as the difference of the total energies $E_{ox} - E_{nox}$, where the index nox corresponds to the nonoxidized complex and the index ox corresponds to the oxidized complex with an unrelaxed geometry.

(33) Pombeiro, A. J. L. *Eur. J. Inorg. Chem.* **1997**, 1473.

(34) Pombeiro, A. J. L. *J. Organomet. Chem.* **2005**, *690*, 6021.

Table 4. Estimated E_L (V vs NHE) and d-Term Values for Benzene, Cymene, Bis(Pyrazol-1yl)acetato, and 4-Acyl-5-pyrazolonato Ligands

Ligand		**Overall E_L**	***d*-term**(a)
	benzene	+1.59	0.795
	cymene	+1.48	0.805
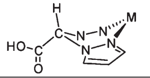	HL^1	+0.73 (b)	0.294
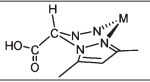	HL^2	+0.66 (c)	0.458
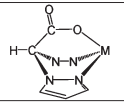	L^1	(+0.57) (d)	0.612
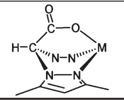	L^2	+0.29 (e)	0.696
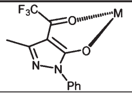	Q^{CF3}	+0.60 (f)	0.667
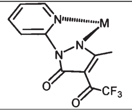	$Q^{py,CF3}$	+0.43 (g)	
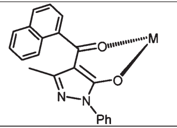	Q^{naph}	+0.40 (h)	0.678
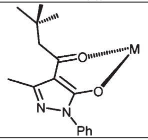	Q^{nPe}	+0.33 (i)	0.694
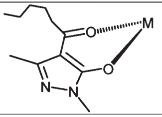	$Q^{Me,nPe}$	+0.27 (j)	0.722

[a] Values are estimated for the theoretically studied complexes and corresponding real or model ligands (see Table 3 and its footnotes). [b] Estimated average from $E^{ox}_{1/2}$ of compounds **3** and **5**. [c] Estimated from $E^{ox}_{1/2}$ of compound **7**. [d] Estimated from $E^{ox}_{p/2}$ of compound **10** (less accurate value). [e] Estimated from $E^{ox}_{1/2}$ of compound **12**. [f] Estimated from $E^{ox}_{1/2}$ (1.82 V vs NHE)[7] of [Ru(η^6-*p*-cymene)(Q^{CF_3})Cl]. [g] Estimated average from $E^{ox}_{1/2}$ of [Ru(η^6-*p*-cymene)(Q^{py,CF_3})Cl] and [Ru(η^6-*p*-cymene)(Q^{py,CF_3})N_3] (1.63 V vs NHE, for both compounds).[7] [h] Estimated from $E^{ox}_{1/2}$ (1.63 V vs NHE)[7] of [Ru(η^6-*p*-cymene)(Q^{naph})Cl]. [i] Estimated average from $E^{ox}_{1/2}$ of [Ru(η^6-*p*-cymene)(Q^{nPe})Cl] and [Ru(η^6-*p*-cymene)(Q^{nPe})N_3] (1.55 and 1.51 V vs NHE, respectively).[7] [j] Estimated from $E^{ox}_{1/2}$ (1.50 V vs NHE)[7] of [Ru(η^6-*p*-cymene)($Q^{Me,nPe}$)Cl].

stronger this character, the lower is E_L). On the basis of the Lever linear relationship (eq 1), valid for octahedral-type complexes, which relates the redox potential (V vs NHE) with the sum of the E_L values for all of the ligands ($\sum E_L$), we propose the estimation of E_L for the bis(pyrazol-1-yl)acetate ligands of this study, as well as for the 4-acyl-5-pyrazolonate ligands we have studied before[31] in related areneruthenium complexes, by assuming that expression 1 is also valid for half-sandwich benzene-type complexes. The slope (S_M) and intercept (I_M) are dependent upon the metal, redox couple, spin state, and stereochemistry, being 0.97 and 0.04 V versus NHE, respectively, for the standard octahedral $Ru^{II/III}$ couple.[27a] The estimated E_L values are collected in Table 4.

$$E = S_M(\Sigma E_L) + I_M/\text{V vs NHE} \qquad (1)$$

Application of eq 1 to the cymene complex [Ru(η^6-*p*-cymene)$Cl_2(PPh_3)$] (**13**; $E^{ox}_{1/2} = +1.39$ V vs NHE), which bears coligands with known E_L values (−0.24 and 0.39 V vs NHE, for Cl^- and PPh_3, respectively),[27a] and assuming that S_M and I_M of the $Ru^{II/III}$ redox pair are maintained (0.97 and 0.04 V vs NHE, respectively), allows us to estimate E_L for the η^6-*p*-cymene ligand (overall value of 1.48 V vs NHE). Following an analogous procedure for [Ru(η^6-benzene)$Cl_2(PPh_3)$] (**14**; $E^{ox}_{1/2} = +1.50$ V vs NHE), the overall E_L value of 1.59 V versus NHE is obtained for the η^6-benzene ligand, which thus behaves as a weaker electron donor than cymene ($E_L = 1.48$ V).

From the knowledge of E_L for cymene and benzene, and applying eq 1 to the appropriate compounds, privileging those that present reversible oxidation waves, it is possible to estimate the following overall E_L values for the bis(pyrazol-1-yl)acetate ligands (ordered according to their overall electron-donor ability): tridentate L^2 (0.29 V) > tridentate

L^1 (0.57 V) > bidentate HL^2 (0.66 V) > bidentate HL^1 (0.73 V). The ligands with dimethylated pyrazolyls are better electron donors than the nonmethylated analogs.

It is also possible to estimate the E_L value for each arm of the ligand, by considering the sum of the arms' contributions (additivity) to the overall E_L. Hence, each pyrazolyl arm in HL^1 contributes +0.36 V to the overall +0.73 V value, whereas, as expected, a lower contribution (+0.33 V) to the overall +0.66 V value of HL^2 is observed for each dimethylpyrazolyl arm, consistent with its stronger electron-donor character.

In a similar way, one can also estimate an average E_L value (−0.27 V) for the carboxylate arm of the tridentate L^1 and L^2, by deducting from their overall E_L values (0.57 and 0.29 V, respectively) the contributions of the pyrazolyl arms (0.73 and 0.66, respectively).

In both HL^1 and HL^2 ligands, each pyrazolyl arm (E_L = 0.36 and 0.33 V) behaves as a weaker electron donor than pyrazole itself (E_L = 0.20 V)[25a] and than each pyrazolyl arm in the tripodal hydrotris(pyrazolyl)methane $HC(pz)_3$ ligand (E_L = 0.14 V)[33] on account of the electron-withdrawing ability of the carboxylic group in the former ligands. The binding carboxylate arm (average E_L of −0.27 V) in the L^1 and L^2 ligands is a much stronger electron donor than the pyrazolyl arms, which is consistent with its negative charge. It is also a more effective donor than acetylacetonate (pentane-2,4-dionate) (E_L= −0.08 V per arm),[27a] being comparable to chloride (E_L= −0.24 V). This is consistent with the proposed[36] E_L value of −0.24 V versus NHE for the ligated carboxylated arm in $[Re(pic)(N_2)(CO)(PPh_3)_2]$ (pic = pyridine-4-carboxylate).

Applying eq 1 to the previously studied[31] series of 4-acyl-5-pyrazolonate cymene-Ru^{II} complexes [Ru(η^6-*p*-cymene)(Q)X] (X = Cl or N_3), and using the above estimated E_L value for cymene, we can also estimate E_L for the bidentate acyl-pyrazolonate (Q) ligand, as shown in Table 4.

All of the studied ligands can then be ordered, according to their electron-donor ability, as follows: $Q^{Me,nPe}$ (anionic O,O-type, with electron-donor alkyl substituents at both the pyrazolyl and the acyl groups) ≈ L^2 (anionic N,N,O-type with alkyl substituents at the pyrazolyl groups) > Q^{nPe} (anionic O,O-type, with an alkyl substituent at the acyl group and an electron-acceptor aromatic substituent at the pyrazolyl group) > Q^{naph} (anionic O,O-type, with electron-acceptor aromatic substituents) > Q^{py,CF_3} (anionic N,N-type, with a pyridyl group and an electron-acceptor CF_3 substituent) > L^1 (anionic N,N, O-type without alkyl substituents) ≈ Q^{CF3} (anionic O, O-type, with the electron-acceptor CF_3 and phenyl substituents) > HL^2 (neutral N,N-type with electron-donor alkyl substituent at the pyrazolyl groups) > HL^1 (neutral N,N-type without alkyl substituents) ≫ cymene (π-benzene with alkyl groups) > π-benzene.

The anionic acyl pyrazolonate ligand $Q^{Me,nPe}$ and the tripodal anionic L^2, both with electron-donor alkyl substituents, are the strongest electron donors, being more effective than the tripodal anionic L^1 (without the alkyl substituents) and Q^{nPe} that bears an electron-acceptor phenyl substituent at the pyrazolyl group. On the other extreme lie the π-arene ligands (benzene and cymene), which are the weakest electron donors, followed, at a great distance, by the other neutral ligands, that is, HL^1 and HL^2 of the N,N-type.

Although the above ordering of the ligands (and of their E_L values) according to their electron-donor character is expected to be reliable, one should be rather cautious with the proposed specific E_L values since they have been estimated by using eq 1 under the assumption that the S_M and I_M values for the octahedral $Ru^{II/III}$ redox couple are also valid for the half-sandwich π-arene $Ru^{II/III}$ complexes. This assumption has to be checked by applying the same general expression to a much wider series of π-benzene (or cymene)-Ru^{II} (or Ru^{III}) complexes, with a variety of coligands with known E_L values.

It is also noteworthy to mention that the approach we have followed for our half-sandwich complexes, based on the standard $Ru^{II/III}$ redox couple, provides an alternative to that proposed by Lever et al.[37] for full-sandwich complexes standardized to the $Fe^{II/III}$ couple.[38] In our case, the E_L values for the benzene (+1.59 V) and cymene (+1.48 V) ligands, at the $Ru^{II/III}$ center, are lower (by 0.27 V) than those (+1.86 and +1.75 V, for benzene and *p*-xylene, respectively)[37] scaled for the $Fe^{II/III}$ redox couple.

Additional and independent information about the electron-donor properties of ligands in complexes may be obtained from the theoretical analysis of orbital interactions using the charge decomposition analysis method.[18] In this method, the M−L bonding nature in a complex [M]L (L, the ligand under study; [M], the rest of the molecule) is considered in terms of MO interactions of two fragments with unrelaxed geometries ({L} and {[M]}). The degree of mixing of the occupied MOs of {L} and the unoccupied MOs of {[M]} upon the fragments' interaction (*d*-term) reflects the ligand-to-metal donation and is presented in Table 4. Although the *absolute* values of the *d*-term have a limited meaning,[39] the term's variation along a series of related ligands is meaningful. In accord, the calculated *d*-term values for the various L ligands of our study correlate well (with the exception of L^1) with those of the E_L parameter, thus confirming the above-mentioned sequence of the donor ability of the ligands. In the case of L^1, the calculations, in contrast with the E_L values, predict a weaker electron-donor ability than that of Q^{CF_3}, but this deviation is conceivably associated to the low accuracy of the estimated E_L value for L_1, based on the oxidation potential of the irreversible wave of **10**. The values of the *d* term for benzene and cymene are not directly comparable with those for pyrazolylacetato and acylpyrazolonato ligands due to the very different nature of the bonding with the metal. However, the higher value for cymene than for benzene is also consistent with the experiment.

---

(35) Alegria, E. C. B.; Martins, L. M. D. R. S.; Guedes da Silva, M. F. C.; Pombeiro, A. J. L. *J. Organomet. Chem.* **2005**, *690*, 1947.

(36) Kirillov, A. M.; Haukka, M.; Guedes da Silva, M. F. C.; Frausto da Silva, J. J. R.; Pombeiro, A. J. L. *J. Organomet. Chem.* **2006**, *691*, 4153.

(37) Lu, S.; Strelets, V. V.; Ryan, M. F.; Pietro, W. J.; Lever, A. B. P. *Inorg. Chem.* **1996**, *35*, 1013.

(38) The basic equation, proposed in ref 34, for mixed sandwich $[FeL_1L_2]$ complexes, is E^0 ($Fe^{II/III}$) = $E_L(L_1) + E_L(L_2)$.

(39) Frenking, G.; Pidun, U. *J. Chem. Soc., Dalton Trans.* **1997**, 1653.

Acknowledgment. This work has been partially supported by the Foundation for Science and Technology (FCT), and its PPCDT programme (FEDER funded), grant SFRH/BD/23187/2005 (R.W.). M.L.K. is grateful to the FCT and IST for a research contract within Ciência 2007 scientific programme. We acknowledge the Universities of Camerino and of Bologna for financial support.

Supporting Information Available: X-ray crystallographic file in CIF format for the X-ray structure determination of **10**. Figures 1S−3S. This material is available free of charge via the Internet at http://pubs.acs.org.